Autophagy functions in lung macrophages and dendritic cells to regulate allergen-dependent inflammatory responses

Neha Dubey[1*], Reilly Woodson[1], Skyler V. Hendrix[1], Anne L. Rosen[2], Rachel L. Kinsella[1#], Samuel R. McKee[1], Marick Starick[1], Nicole Rivera-Espinal[1], Sumanta K. Naik[1], Asya Smirnov[1], Darren Kreamalmeyer[1], Andrew L. Kau[2], Christina L. Stallings[1*]

[1]Department of Molecular Microbiology and Center for Women's Infectious Disease Research, Washington University School of Medicine, St. Louis, MO 63110, USA

[2]Division of Allergy and Immunology, Department of Medicine and Center for Women's Infectious Disease Research, Washington University School of Medicine, St. Louis, MO 63110, USA

[#]Current address: Department of Medicine, Division of Infectious Diseases and Emory Vaccine Center, Emory University School of Medicine, Atlanta, GA 30329, USA.

*Correspondence: stallings@wustl.edu, nehadubey@wustl.edu

Keywords: asthma, allergy, autophagy, inflammation, eosinophils, neutrophils, T cells, T_H17

ABSTRACT

Asthma affects 260 million people worldwide, with severe asthma cases that are associated with T_H17/T_H1 responses and neutrophil dominated inflammation being the most difficult to treat due to corticosteroid insensitivity. Single nucleotide polymorphisms in the *ATG5* gene, which encodes for a protein required for the cellular recycling process of autophagy, are associated with higher risk for developing severe asthma. However, the role for ATG5 during allergic inflammation remains mostly unknown. We have identified an autophagy-dependent role for ATG5 in lung macrophages and dendritic cells (DCs) for suppressing T_H17 responses and neutrophil accumulation in house dust mite (HDM)-challenged mice, a T_H17/T_H1 dominated model for allergic airway inflammation due to contamination of the HDM with lipopolysaccharide. In

32 contrast, autophagy was required to promote eosinophil accumulation in the T_H2-dominated
33 ovalbumin model of allergic airway inflammation, supporting a model where autophagy functions
34 in lung macrophages and DCs to suppress T_H17 responses and promote T_H2 responses in an
35 allergen-dependent manner. In addition, we discover that autophagy is also required in
36 macrophages exposed to HDM to suppress the secretion of cytokines and chemokines that would
37 otherwise recruit neutrophils to the lungs, independent of T cell responses. Together, our data
38 identify multiple roles for autophagy in suppressing the neutrophil accumulation in lungs that is
39 associated with severe asthma.
40

41 **INTRODUCTION**

42 Asthma affects nearly 260 million people worldwide[1] and involves a deleterious inflammatory
43 response that results in immune cell infiltration in the lungs, bronchoconstriction, airway
44 remodeling, and airway hyperresponsiveness (AHR)[2]. Asthma and allergic airway inflammation
45 occurs in response to a wide variety of substances called allergens that induce varying levels of
46 immune hypersensitivity[3]. The most prevalent form of asthma is associated with T_H2 responses
47 signaled through airway epithelial cell-derived alarmins IL-33 and IL-25, which stimulate the
48 production of IL-4, IL-5, IL-13, and TGF-β cytokines by airway cells and an influx of eosinophils
49 and mast cells, along with other inflammatory cells, into the lungs[4–6]. Although this form of the
50 disease is usually less severe and responsive to conventional corticosteroid therapy[4], asthma can
51 also present with other distinct immunological and pathological features[7–9]. In particular, 5-
52 15% of the total asthma cases involve a T_H17-dominated response, leading to neutrophil
53 recruitment and accumulation in the lungs[10,11]. Increased accumulation of neutrophils is
54 associated with severe asthma[10,11], which is clinically defined by resistance to corticosteroid
55 therapy[8,12–14]. In addition, T_H1 responses mediated by interferon-γ (IFN-γ) production by
56 $CD4^+$ T cells are also associated with severe asthma cases[15,16]. The association of heightened
57 T_H17 responses, T_H1 responses, and neutrophil accumulation with AHR and corticosteroid
58 resistance has been reported during severe asthma in both mice and humans[14–17].

59 A better understanding of the immunological processes that contribute to severe asthma is
60 required to develop alternative therapies for when corticosteroids fail. Several studies attempting
61 to map genetic associations with asthma have identified a link between the *ATG5* gene and
62 susceptibility to severe asthma. A single nucleotide polymorphism (SNP) in the third intron of the

63 *ATG5* gene (rs12212740, alleles G/A, minor variant: G) was associated with lower pre-
64 bronchodilator forced expiratory volume (FEV1) and a risk of moderate to severe asthma in non-
65 Hispanic Caucasian children[18]. In a separate genome wide association study, a SNP in the 5'
66 untranslated region (UTR)/annotated promoter region of the *ATG5* gene (rs510432, alleles G/A,
67 minor variant: G) was associated with increased risk of asthma in children[19]. The G variant allele
68 of SNP rs510432 results in increased promoter activity and higher expression of *ATG5* mRNA in
69 nasal mucosal cells isolated from the children with acute asthma compared to non-acute and
70 healthy controls. Another study reported the association of the G variant allele of SNP rs510432
71 with increased sputum neutrophil counts in adult asthma patients, establishing a correlation
72 between dysregulated *ATG5* expression and neutrophil recruitment during asthma[20].
73 ATG5 is essential for the process of autophagy, which involves multiple protein complexes
74 that target cytosolic components and organelles to the lysosome for degradation[21–23]. The
75 ULK1 complex (ULK1/ULK2, ATG13, FIP200, ATG101) and PI3 kinase complex (ATG14,
76 BECLIN1, VPS15, and VPS34) initiate autophagy by generating a phagophore from the
77 membranes of the endoplasmic reticulum[24,25]. Elongation of the autophagosomal double
78 membrane depends on two ubiquitin-like conjugation systems. In the first system, ATG12 is
79 activated by ATG7, transferred to ATG10, and covalently attached to ATG5. In the second system,
80 LC3 (microtubule-associated protein 1 light chain 3) is conjugated to phosphatidylethanolamine
81 to generate the membrane bound form LC3-II through the actions of ATG7, ATG3, and the ATG5-
82 ATG12/ATG16L complex[25,26]. The autophagosome membrane is then completed and targeted
83 for fusion with the lysosome, where the autophagosome cargo are degraded. Several studies have
84 reported that the expression of genes required for autophagy, including *ATG5*, are elevated in the
85 lungs of asthma patients compared to non-asthmatic individuals[27–29]. Furthermore, LC3-II
86 expression is increased in the sputum granulocytes from severe asthma patients compared to non-
87 severe asthma patients[20,30]. Despite the genetic associations of ATG5 and autophagy with
88 severe asthma, the precise roles for autophagy during asthma have remained elusive. Several
89 experimental studies have implicated both deleterious and protective functions of autophagy
90 during asthma[31], creating uncertainty in the field. There are likely multiple contributors to the
91 discrepancies. For example, in most of the experimental studies so far, the interpretations were
92 largely made based on pleiotropic chemical treatments that impact autophagy, among other
93 pathways[32–38]. In addition, autophagy likely plays cell-type specific roles during exposure to

94 allergens, which may complicate studies that use chemical treatments or globally knockdown
95 autophagy gene expression[14].
96 Innate immune cells are a primary contributor to lung inflammation during asthma and
97 ATG5 has been shown to function both dependent and independent of autophagy to regulate
98 inflammatory responses in innate immune cells during infection[21,22,39–42]. However, studies
99 into the roles for autophagy specifically in innate immune cells during asthma and allergic airway
100 inflammation have been limited. In the one study that focused on ATG5 in innate immune cells,
101 loss of *Atg5* in hematopoietic cells was sufficient to cause increased neutrophils and macrophages
102 in bronchoalveolar lavages (BAL), increased AHR, and higher levels of IL-17 and IL-1β in
103 response to house dust mites (HDM) challenge in mice[14]. When *Atg5*-deficient bone marrow
104 cells were cultured in the presence of GM-CSF to generate a mixed culture of dendritic cells (DCs),
105 macrophages, and granulocytes, and treated with HDM, the cells produced higher levels of IL-1α,
106 IL-1β, IL-23, and caspase-1 as compared to wild type (WT) GM-CSF cultures. *Atg5*$^{-/-}$ GM-CSF
107 cultures also caused a higher level of IL-17 production in a co-culture with CD4^{+} T cells as
108 compared to WT GM-CSF cultures. Transfer of *Atg5*$^{-/-}$ GM-CSF cultured cells loaded with HDM
109 into WT mice intratracheally resulted in increased neutrophilic inflammation and IL-17 production
110 as compared to transfer of WT GM-CSF cultured cells, indicating that ATG5 is important to
111 control neutrophil recruitment in response to HDM exposure. These studies support a role for
112 ATG5 in innate immune cells to control neutrophilic inflammation during allergic challenge.
113 However, it is still unknown which innate immune cell types specifically require ATG5 and
114 whether its role in controlling neutrophilic inflammation during allergic challenge is dependent on
115 autophagy, since ATG5 and other autophagy proteins have been shown to function outside of
116 autophagy to regulate inflammation[21,23,41,42]. To address these gaps in understanding, we used
117 genetic tools to dissect the autophagy-dependent and independent roles for ATG5 in specific innate
118 immune cells in two allergic airway inflammation mice models. We find that autophagy is
119 specifically required in CD11c^{+} lung macrophages and DCs to shift the balance away from T_H17
120 responses and towards T_H2 responses in an allergen-dependent manner. In addition, autophagy
121 functions in macrophages in a T cell-independent manner to suppress pathogen associated
122 molecular pattern (PAMP)-triggered cytokine and chemokine production that would otherwise
123 recruit neutrophils to the lung. Thus, autophagy impacts multiple different processes within innate
124 immune cells that are important for regulating inflammation in response to exposure to allergens.

125

126 **RESULTS**

127 **ATG5 is required in LysM$^+$ cells to promote eosinophilia and to suppress neutrophilia in**
128 **airways following allergen exposure**

129 The role of ATG5 and autophagy in specific innate immune cell types during asthma has yet to be
130 tested since all prior work was done with general administration of pleiotropic and non-cell type
131 specific treatments[28,32,36,37] or using cell cultures containing a mixed population of cell
132 types[14]. To determine if ATG5 functions in innate immune cells during allergic airway
133 inflammation, we used *Atg5$^{fl/fl}$-LysM-Cre* mice[21,39,43,44], which specifically delete *Atg5* in
134 monocytes, macrophages, neutrophils, and some DCs. Flow cytometric analysis of the immune
135 cell populations in the naïve mouse lungs showed that the only cell type that was significantly
136 different in its abundance in the *Atg5$^{fl/fl}$-LysM-Cre* and *Atg5$^{fl/fl}$* mice was a higher number of non-
137 alveolar macrophages in the lungs *Atg5$^{fl/fl}$-LysM-Cre* mice compared to the *Atg5$^{fl/fl}$* mice (**Figure**
138 **S1A**). Whereas, the numbers of neutrophils, eosinophils, alveolar macrophages, DCs,
139 inflammatory monocytes, naïve CD4$^+$ T cells (CD44$^-$CD62L$^+$), activated CD4$^+$ T cells
140 (CD44$^+$CD62L$^-$), regulatory T cells (T_{regs}) (CD4$^+$CD25$^+$), and CD8$^+$ T cells were similar between
141 the between *Atg5$^{fl/fl}$-LysM-Cre* and *Atg5$^{fl/fl}$* mice (**Figure S1A**). To determine the role of ATG5
142 during allergic airway inflammation, we performed an ovalbumin (OVA) induced allergic airway
143 inflammation model[45] (**Figure 1A**), which induces a T_H2-dominanted allergic inflammatory
144 response in lungs. We sensitized the *Atg5$^{fl/fl}$-LysM-Cre* mice and *Atg5$^{fl/fl}$* control mice by
145 intraperitoneal (i.p.) administration of 50 μg purified OVA coupled with an aluminum potassium
146 sulfate adjuvant (alum) on days 0, 7, and 14, before challenging the mice intranasally (i.n.) with 1
147 mg OVA on days 20, 21, and 22. Analysis of the immune cell populations in the lungs on day 23
148 compared to naïve mice confirmed that both eosinophils and neutrophils were recruited to the
149 lungs in response to the OVA challenge, but the inflammatory response to OVA challenge was
150 dominated by eosinophils in the *Atg5$^{fl/fl}$* mice (**Figures 1B-C, S1A**), as would be expected in a T_H2
151 dominant model. There was no difference in the number of neutrophils in the lungs of OVA-
152 challenged *Atg5$^{fl/fl}$-LysM-Cre* and *Atg5$^{fl/fl}$* mice (**Figure 1C**). However, OVA-challenged *Atg5$^{fl/fl}$-*
153 *LysM-Cre* mice accumulated significantly lower numbers of eosinophils in the lungs compared to
154 *Atg5$^{fl/fl}$* mice (**Figures 1B-C**), suggesting a shift away from T_H2 responses. OVA-challenged
155 *Atg5$^{fl/fl}$-LysM-Cre* mice also accumulated significantly lower numbers of non-alveolar

156 macrophages, DCs, and $CD4^+$ T cells in the lungs compared to OVA-challenged *Atg5*$^{fl/fl}$ mice
157 (**Figure 1C**). There were no differences in the number of alveolar macrophages, inflammatory
158 monocytes, B cells, $CD8^+$ T cells, and T_{regs} in the lungs of OVA-challenged *Atg5*$^{fl/fl}$*-LysM-Cre* and
159 *Atg5*$^{fl/fl}$ mice (**Figure S1B)**. We also analyzed immune cell accumulation specifically in the
160 airways by instilling a fluorescently labeled αCD45.2 antibody into the airways before analysis by
161 flow cytometry. The airways of OVA-challenged *Atg5*$^{fl/fl}$*-LysM-Cre* mice contained significantly
162 fewer eosinophils and a higher number of neutrophils and B cells compared to OVA-challenged
163 *Atg5*$^{fl/fl}$ mice (**Figures 1D, S1C)**, whereas the number of the other immune cell types analyzed
164 were similar between OVA-challenged *Atg5*$^{fl/fl}$*-LysM-Cre* and *Atg5*$^{fl/fl}$ mice (**Figure S1C**).
165
166 The data from OVA-challenged *Atg5*$^{fl/fl}$*-LysM-Cre* and *Atg5*$^{fl/fl}$ mice indicates that ATG5 is
167 required in $LysM^+$ cells to promote eosinophilia and suppress neutrophilia in the airways during a
168 T_H2-dominated allergic inflammatory response. To determine how ATG5 would impact immune
169 responses in a T_H17/T_H1-dominated model for allergic airway inflammation, we used an intranasal
170 HDM challenge model where lipopolysaccharide (LPS) contamination of the HDM has been
171 shown to drive a primarily T_H17/T_H1-dominated response[46–48]. In this model, which is similar
172 to as used in the prior study that exposed tamoxifen inducible global *Atg5*$^{-/-}$ mice to HDM and
173 reported increased neutrophilic inflammation in the airways of *Atg5*$^{-/-}$ mice[14], HDM
174 administered intranasally is sensed directly by innate immune cells in the lung through several
175 pattern recognition receptors[49–51]. In addition, residual LPS contamination in the HDM is
176 sensed by TLR4 and the DerP2 antigen in HDM mimics MD2, a TLR4 co-stimulatory molecule
177 that confers hypersensitivity to LPS, together skewing T cell responses towards a T_H1/T_H17
178 response[46,47,52]. We challenged the *Atg5*$^{fl/fl}$*-LysM-Cre* and *Atg5*$^{fl/fl}$ mice with HDM intranasally
179 on days 0, 7 and 14 before analyzing immune cell infiltrates in the lungs and airways on day 15
180 by flow cytometry **(Figure 1E)**. HDM challenge resulted in the accumulation of a higher number
181 of neutrophils than eosinophils in the lungs and airways of both *Atg5*$^{fl/fl}$*-LysM-Cre* and *Atg5*$^{fl/fl}$
182 mice **(Figures 1F-H, S1A)**, consistent with HDM eliciting a T_H17/T_H1-dominated allergic airway
183 inflammatory response. Unlike in the T_H2-dominated OVA model, there was no difference in the
184 number of eosinophils that accumulated in the lungs or airways of HDM-challenged *Atg5*$^{fl/fl}$*-LysM-*
185 *Cre* and *Atg5*$^{fl/fl}$ mice **(Figure 1G-H)**. In contrast, HDM-challenged *Atg5*$^{fl/fl}$*-LysM-Cre* mice
186 accumulated significantly more neutrophils in the lungs and airways than HDM-challenged *Atg5*$^{fl/fl}$

187 controls **(Figures 1F-H)**. HDM challenge of *Atg5$^{fl/fl}$-LysM-Cre* mice also resulted in the
188 accumulation of significantly more non-alveolar macrophages, DCs, inflammatory monocytes,
189 activated CD4$^+$ T cells, and T_{regs} in the lungs as compared to *Atg5$^{fl/fl}$* controls **(Figures 1G)**,
190 although the numbers of non-alveolar macrophages, DCs, inflammatory monocytes, activated
191 CD4$^+$ T cells, and T_{regs} in the airways of OVA-challenged *Atg5$^{fl/fl}$-LysM-Cre* and *Atg5$^{fl/fl}$* mice were
192 similar (**Figure S1D**). There were no differences in the numbers of alveolar macrophages, B cells,
193 naïve CD4$^+$ T cells, and CD8$^+$ T cells in the lungs or airways of HDM-challenged *Atg5$^{fl/fl}$-LysM-*
194 *Cre* and *Atg5$^{fl/fl}$* mice **(Figure S1D-E).** Together, these data indicate that loss of ATG5 expression
195 in LysM$^+$ cells results in an enhanced inflammatory response to HDM challenge. Indeed, when we
196 performed histological analysis with hematoxylin and eosin (H&E) staining of lung sections from
197 the HDM challenged *Atg5$^{fl/fl}$-LysM-Cre* and *Atg5$^{fl/fl}$* mice, we observed a greater area of cellular
198 infiltrate in the lungs of HDM-challenged *Atg5$^{fl/fl}$-LysM-Cre* mice compared to *Atg5$^{fl/fl}$* mice
199 (**Figures 1I-J, S1F**), supportive of an increased inflammatory response in the lungs.
200
201 The heightened neutrophil-dominated inflammatory response in the airways of HDM-challenged
202 *Atg5$^{fl/fl}$-LysM-Cre* mice suggests that the mice are experiencing a more severe allergic reaction to
203 the HDM. A characteristic feature of airway allergic reactions is the accumulation of mucus in the
204 lungs, which increases with the severity of the allergic reaction[53]. We assessed the accumulation
205 of neutral mucins (glycoproteins in mucus) in the airways of the HDM-challenged mice by staining
206 with the periodic acid-schiff (PAS) dye and observed that a significantly greater area of the lung
207 was PAS positive in HDM-challenged *Atg5$^{fl/fl}$-LysM-Cre* mice compared to *Atg5$^{fl/fl}$* controls
208 (**Figures 1K-L, S1G).** Therefore, the lung pathology in HDM-challenged *Atg5$^{fl/fl}$-LysM-Cre* mice
209 is consistent with a more severe airway allergic reaction. These data demonstrate that ATG5
210 expression is required in LysM$^+$ cells to suppress neutrophil-dominated inflammation in the
211 airways of mice challenged with HDM.
212
213 **ATG5 expression in innate immune cells promotes T_H2 responses and suppresses T_H17**
214 **responses during allergic airway inflammation**
215 Eosinophil and neutrophil recruitment to the airways following allergen exposure is generally
216 associated with T_H2 and T_H17/T_H1 mediated immune responses, respectively[9,46,52,54]. We
217 investigated whether the differences in eosinophil and neutrophil recruitment to the airways of

218 allergen challenged *Atg5*$^{fl/fl}$*-LysM-Cre* and *Atg5*$^{fl/fl}$ mice reflected variances in the numbers of T_H2
219 versus T_H17 and T_H1 cells by analyzing the expression of transcription factors that are associated
220 with specific CD4$^+$ T helper cell subsets. Specifically, we identified the CD4$^+$ T cell populations
221 expressing RORγt, GATA3, or T-bet by flow cytometry to quantify T_H17, T_H2, and T_H1 cells,
222 respectively. Similar to our prior analyses **(Figure 1C)**, the lungs of OVA-challenged *Atg5*$^{fl/fl}$-
223 *LysM-Cre* mice contained significantly fewer CD4$^+$ T cells compared to OVA-challenged *Atg5*$^{fl/fl}$
224 mice (**Figure 2A**), where specifically the numbers of GATA3$^+$ and T-bet$^+$, but not RORγt$^+$, CD4$^+$
225 T cells were significantly lower in the lungs of the OVA-challenged *Atg5*$^{fl/fl}$*-LysM-Cre* mice
226 compared to OVA-challenged *Atg5*$^{fl/fl}$ mice (**Figure 2B**). Therefore, the decreased number of
227 eosinophils recruited to the airways of OVA-challenged *Atg5*$^{fl/fl}$*-LysM-Cre* mice compared to
228 OVA-challenged *Atg5*$^{fl/fl}$ mice **(Figure 1B-D)** correlates with a decreased number of T_H2 and T_H1
229 cells in the lungs of *Atg5*$^{fl/fl}$*-LysM-Cre* mice.
230
231 The significantly increased numbers of CD4$^+$ T cells in the lungs of HDM-challenged *Atg5*$^{fl/fl}$-
232 *LysM-Cre* mice compared to HDM-challenged *Atg5*$^{fl/fl}$ mice (**Figures 1G, 2C**) was comprised of
233 significantly higher numbers of RORγt$^+$ CD4$^+$ T cells (**Figure 2D**), without differences in the
234 numbers of GATA3$^+$ or T-bet$^+$ CD4$^+$ T cells between the genotypes (**Figure 2D**). Thus, the
235 increased number of neutrophils recruited to the airways of HDM-challenged *Atg5*$^{fl/fl}$*-LysM-Cre*
236 mice compared to HDM-challenged *Atg5*$^{fl/fl}$ mice **(Figure 1B-D)** correlates with an increased
237 number of T_H17 cells in the lungs of *Atg5*$^{fl/fl}$*-LysM-Cre* mice. To specifically determine if the
238 increased accumulation of neutrophils and RORγt$^+$ CD4$^+$ T cells in lungs of HDM-challenged
239 *Atg5*$^{fl/fl}$*-LysM-Cre* mice was accompanied by increased IL-17 expression from T cells, we crossed
240 the *Atg5*$^{fl/fl}$*-LysM-Cre* and *Atg5*$^{fl/fl}$ mice with an IL-17 reporter mouse[55] (*Il17a*^{eGFP}, Jackson
241 Laboratory) that expresses GFP as a proxy of IL-17, generating *Atg5*$^{fl/fl}$*-LysM-Cre/Il17a*^{eGFP} and
242 *Atg5*$^{fl/fl}$/*Il17a*^{eGFP} mice. Following HDM challenge, we detected a similar increase in the abundance
243 of neutrophils and activated CD4$^+$ T cells in *Atg5*$^{fl/fl}$*-LysM-Cre/Il17a*^{eGFP} mice compared to
244 *Atg5*$^{fl/fl}$/*Il17a*^{eGFP} controls (**Figure 2E**) as observed in the *Atg5*$^{fl/fl}$*-LysM-Cre* and *Atg5*$^{fl/fl}$ parent
245 strains **(Figures 1E-F).** We monitored GFP expression from immune cells following HDM
246 challenge of *Atg5*$^{fl/fl}$*-LysM-Cre/Il17a*^{eGFP} and *Atg5*$^{fl/fl}$/*Il17a*^{eGFP} mice using flow cytometry and
247 found that the only cell types positive for GFP were CD4$^+$ T cells. A higher percentage of total
248 CD4$^+$ T cells, activated CD4$^+$ T cells, and T_{regs} expressed GFP in HDM-challenged *Atg5*$^{fl/fl}$*-LysM-*

249 *Cre/Il17a*^{eGFP} mice compared to *Atg5*$^{fl/fl}$/*Il17a*^{eGFP} mice **(Figure 2F)**, which reflected a higher
250 number of GFP^{+} activated CD4^{+} T cells and T_{regs} in the lungs of HDM-challenged *Atg5*$^{fl/fl}$*-LysM-*
251 *Cre/Il17a*^{eGFP} mice compared to HDM-challenged *Atg5*$^{fl/fl}$/*Il17a*^{eGFP} controls **(Figure 2G)**. Based
252 on mean fluorescence intensity (MFI), the activated CD4^{+} T cells in *Atg5*$^{fl/fl}$*-LysM-Cre/Il17a*^{eGFP}
253 mice also expressed more GFP and, as a proxy, IL-17 per cell than activated CD4^{+} T cells from
254 *Atg5*$^{fl/fl}$/*Il17a*^{eGFP} mice following HDM challenge **(Figure 2H)**. These data indicate that loss of
255 *Atg5* in LysM^{+} cells results in increased IL-17 expression from activated CD4^{+} T cells, likely
256 reflecting the increased number of RORγt^{+} CD4^{+} T cells. A higher T_H17/T_{reg} ratio is also associated
257 with increased asthma severity, increased AHR, and corticosteroid-refractory asthma[56–60].
258 Indeed, we observed an increased ratio of IL-17^{+} CD4^{+} T cells to T_{regs} in HDM-challenged *Atg5*$^{fl/fl}$-
259 *LysM-Cre/Il17a*^{eGFP} mice compared to HDM-challenged *Atg5*$^{fl/fl}$/*Il17a*^{eGFP} controls **(Figure 2I)**,
260 supporting that loss of *Atg5* in myeloid cells results in a CD4^{+} T cell imbalance that is associated
261 with increased asthma severity[56,57,59]. Together, our data demonstrate that ATG5 is required
262 in innate immune cells to promote T_H2 responses in OVA-challenged mice and to suppress T_H17
263 responses in HDM-challenged mice.
264

265 **Increased T_H17 responses in HDM-challenged *Atg5*$^{fl/fl}$*-LysM-Cre* mice are partially**
266 **responsible for the increased neutrophil accumulation**

267 To investigate how ATG5 regulates inflammatory responses during exposure to airway allergens,
268 we further dissected the role for ATG5 in the HDM challenge model. Given the association of
269 T_H17 responses with increased neutrophil accumulation during asthma, we investigated whether
270 the increased T_H17 responses in the lungs of HDM-challenged *Atg5*$^{fl/fl}$*-LysM-Cre* mice contributed
271 to the accompanying increased neutrophil accumulation. To investigate the role of T cells in the
272 neutrophil accumulation, we depleted T cells in HDM-challenged *Atg5*$^{fl/fl}$*-LysM-Cre* and *Atg5*$^{fl/fl}$
273 mice by administering 250 µg each of αCD4 and αCD8 neutralizing antibodies intraperitoneally
274 2 days before (day -2) the first HDM challenge and again on days 5 and 12 post the initial HDM
275 challenge (**Figure 3A**). Separate groups of HDM-challenged mice received 500 µg of isotype
276 control antibodies on the same schedule to serve as controls. Flow cytometric analysis of immune
277 cell populations in the lungs at 15 days following the first HDM dose confirmed efficient T cell
278 depletion in the *Atg5*$^{fl/fl}$*-LysM-Cre* and *Atg5*$^{fl/fl}$ mice treated with αCD4 and αCD8 antibodies
279 (**Figure 3B**). Similar to prior experiments **(Figures 1F-G)**, HDM-challenged *Atg5*$^{fl/fl}$*-LysM-Cre*

280 mice that received the isotype control antibody accumulated higher numbers of neutrophils in the
281 lungs compared to HDM-challenged *Atg5*$^{fl/fl}$ mice that received the isotype control (**Figure 3C**).
282 T cell depletion significantly decreased the number of neutrophils in the lungs of HDM-challenged
283 *Atg5*$^{fl/fl}$*-LysM-Cre* mice (**Figure 3C**), demonstrating that T cells contribute to the neutrophil
284 accumulation in HDM-challenged *Atg5*$^{fl/fl}$*-LysM-Cre* mice. However, even after T cell depletion,
285 the neutrophil numbers were still higher in the lungs of HDM-challenged *Atg5*$^{fl/fl}$*-LysM-Cre* mice
286 than observed in the lungs of HDM-challenged *Atg5*$^{fl/fl}$ mice (**Figure 3C**). These data suggest that
287 although T cells contribute to neutrophil accumulation in response to HDM challenge, there exists
288 a T cell-independent process that also promotes neutrophil accumulation in the lungs of HDM-
289 challenged *Atg5*$^{fl/fl}$*-LysM-Cre* mice.
290
291 To investigate the effects of T cell depletion on T_H1, T_H2, and T_H17 responses, we monitored the
292 levels of IFN-γ, IL-5, and IL-17, respectively, in the lungs of HDM-challenged *Atg5*$^{fl/fl}$*-LysM-Cre*
293 and *Atg5*$^{fl/fl}$ mice following T cell depletion versus treatment with isotype control antibodies.
294 Within the isotype control antibody treated groups, we observed significantly higher levels of IL-
295 17 in the lungs of HDM-challenged *Atg5*$^{fl/fl}$*-LysM-Cre* mice compared to the *Atg5*$^{fl/fl}$ controls
296 (**Figure 3D**), but no differences in the levels of IFN-γ and IL-5 (**Figure 3E, F**). This is consistent
297 with the higher number of RORγt$^+$ T_H17 cells, but no differences in the numbers of GATA3$^+$ T_H2
298 or T-bet$^+$ T_H1 cells, in the lungs of HDM-challenged *Atg5*$^{fl/fl}$*-LysM-Cre* mice compares to HDM-
299 challenged *Atg5*$^{fl/fl}$ mice **(Figure 2D)**. T cell depletion significantly reduced the elevated IL-17
300 levels in the lungs of HDM-challenged *Atg5*$^{fl/fl}$*-LysM-Cre* mice to the levels observed in the HDM-
301 challenged *Atg5*$^{fl/fl}$ mice **(Figure 3D).** Consistent with the data from the *Atg5*$^{fl/fl}$*-LysM-*
302 *Cre/Il17a*^{eGFP} mice **(Figure 2),** these studies support that T cells are the primary source of IL-17
303 during HDM challenge and indicate that ATG5 specifically suppresses T_H17 responses in response
304 to HDM challenge. T cell depletion also reduced the levels of IFN-γ in the lungs of HDM-
305 challenged *Atg5*$^{fl/fl}$ mice to below the limit of detection, but did not affect the IFN-γ levels in the
306 HDM-challenged *Atg5*$^{fl/fl}$*-LysM-Cre* mice (**Figure 3E).** These data suggest that while T cells are
307 the major source of IFN-γ in HDM-challenged *Atg5*$^{fl/fl}$ mice, IFN-γ is produced independently of
308 T cells in HDM-challenged *Atg5*$^{fl/fl}$*-LysM-Cre*.
309

310 The T cell depletion studies indicate that enhanced T_H17 responses contribute to the enhanced
311 neutrophil accumulation in the lungs of HDM-challenged *Atg5$^{fl/fl}$-LysM-Cre* mice. To directly
312 examine the role of IL-17 signaling, we intraperitoneally administered 100 µg of an antibody that
313 binds and blocks IL-17 1 day before the first HDM challenge (day -1) and again on days 1, 3, 5,
314 6, 8, 10, 12, and 13 following the initial HDM challenge (**Figure 3G).** Separate groups of HDM-
315 challenged mice received 100 µg of isotype control antibodies on the same schedule to serve as
316 controls. Blocking IL-17 signaling significantly reduced the number of neutrophils accumulating
317 in the lungs of HDM-challenged *Atg5$^{fl/fl}$-LysM-Cre* mice **(Figure 3H)**, to a similar degree as
318 observed during T cell depletion in HDM-challenged *Atg5$^{fl/fl}$-LysM-Cre* mice **(Figure 3C).** This
319 supports that elevated T_H17 responses contribute to increased neutrophil accumulation in the lungs
320 of HDM-challenged *Atg5$^{fl/fl}$-LysM-Cre* mice. However, similar to as observed during T cell
321 depletion **(Figure 3C)**, the neutrophil numbers remained higher in the lungs of HDM-challenged
322 *Atg5$^{fl/fl}$-LysM-Cre* mice than observed in HDM-challenged *Atg5$^{fl/fl}$* mice following αIL-17
323 treatment **(Figure 3H)**. Therefore, ATG5 inhibits neutrophil accumulation during HDM challenge
324 in part through suppressing T_H17 responses, but also through another T cell-independent
325 mechanism.
326
327 **ATG5 is required in macrophages to control the expression of neutrophil recruitment signals**
328 **during exposure to HDM**
329 A T cell-independent inflammatory process that is negatively regulated by autophagy in innate
330 immune cells is inflammasome activation[61–63]. Several reports have demonstrated a role for the
331 NLRP3 (nucleotide-binding oligomerization domain-like Receptor Family Pyrin Domain
332 Containing 3) inflammasome pathway, which catalyzes caspase-1 dependent release of pro-
333 inflammatory cytokines IL-1β and IL-18, during severe allergic inflammation[64–67]. In addition,
334 *Atg5$^{-/-}$* bone marrow cells cultured in GM-CSF produce higher levels of IL-1β than wild-type
335 cultures following exposure to HDM *in vitro*[14]. We measured the levels of IL-1β in the lungs of
336 HDM-challenged *Atg5$^{fl/fl}$-LysM-Cre* and *Atg5$^{fl/fl}$* mice and although there was a trend of higher
337 levels of IL-1β in the HDM-challenged *Atg5$^{fl/fl}$-LysM-Cre* mice, the IL-1β levels were not
338 significantly different than in HDM-challenged *Atg5$^{fl/fl}$* mice (**Figure S2A**). To directly interrogate
339 if the increased neutrophil accumulation following HDM challenge is a consequence of
340 inflammasome activation in the absence of autophagy in *Atg5$^{fl/fl}$-LysM-Cre* mice, we crossed the

341 *Atg5*$^{fl/fl}$*-LysM-Cre* and *Atg5*$^{fl/fl}$ mice with *Casp1/11*$^{-/-}$ mice (Jackson Laboratory), which are deleted
342 for the genes encoding caspase-1 and caspase-11. We challenged *Atg5*$^{fl/fl}$*-LysM-Cre/Casp1/11*$^{-/-}$
343 and *Atg5*$^{fl/fl}$*/Casp1/11*$^{-/-}$ mice with HDM and analyzed the lung immune cell populations. Similar
344 to *Atg5*$^{fl/fl}$*-LysM-Cre* mice, the lungs of HDM-challenged *Atg5*$^{fl/fl}$*-LysM-Cre/Casp1/11*$^{-/-}$ mice
345 accumulated more neutrophils, non-alveolar macrophages, DCs, activated $CD4^+$ T cells, and T_{regs}
346 than *Atg5*$^{fl/fl}$/Casp1/*11*$^{-/-}$ mice, with no differences in the number of eosinophils **(Figure S2B)**.
347 Deletion of *Casp1* and *Casp11* also did not alter the non-significant trends in IL-1β levels in the
348 lungs of HDM-challenged *Atg5*$^{fl/fl}$*-LysM-Cre* and *Atg5*$^{fl/fl}$ mice **(Figure S2C)**. These data indicate
349 that neutrophils accumulate in the lungs of HDM-challenged *Atg5*$^{fl/fl}$*-LysM-Cre* mice independent
350 of caspase-1 and caspase-11.
351
352 To explore the T cell and inflammasome-independent mechanism by which ATG5 regulates
353 neutrophil accumulation during HDM exposure, we examined the inflammatory signals that
354 remained higher in the lungs of HDM-challenged *Atg5*$^{fl/fl}$*-LysM-Cre* mice compared to HDM-
355 challenged *Atg5*$^{fl/fl}$ mice during T cell depletion using a cytokine bead array **(Figures 4A, S2D)**.
356 We found that the levels of G-CSF (granulocyte colony stimulating factor), KC (IL-8), IL-1α, IL-
357 12p40, and MIP-1α were higher in the lungs of HDM-challenged *Atg5*$^{fl/fl}$*-LysM-Cre* mice
358 compared to HDM-challenged *Atg5*$^{fl/fl}$ mice when T cells were depleted (**Figures 4A**). G-CSF is a
359 cytokine important for neutrophil development, KC is a neutrophil chemoattractant, and IL-1α,
360 IL-12p40, and MIP-1α have all been associated with neutrophil recruitment during inflammation
361 [68–71]. The higher levels of G-CSF, KC, IL-1α, IL-12p40, MIP-1α, and IFN-γ in HDM-
362 challenged *Atg5*$^{fl/fl}$*-LysM-Cre* mice depleted for T cells (**Figures 3E, 4A)** implies that the source
363 of these inflammatory signals may be an innate immune cell.
364
365 *Atg5*$^{fl/fl}$*-LysM-Cre* mice delete *Atg5* in multiple different types of innate immune cells, including
366 neutrophils, macrophages, inflammatory monocytes, and some DCs. To determine if ATG5
367 functioned specifically in macrophages to suppress neutrophil accumulation during HDM-
368 challenge, we challenged *Atg5*$^{fl/fl}$*-CD11c-Cre* (delete *Atg5* in lung macrophages and DCs) with
369 HDM and monitored lung inflammatory responses. Similar to as observed in HDM-challenged
370 *Atg5*$^{fl/fl}$*-LysM-Cre* mice **(Figure 1)**, the lungs of HDM-challenged *Atg5*$^{fl/fl}$*-CD11c-Cre* mice
371 accumulated higher numbers of neutrophils, non-alveolar macrophages, DCs, inflammatory

372 monocytes, activated $CD4^+$ T cells, and T_{regs} with no difference in the number of eosinophils
373 (**Figure 4B**) as compared to HDM-challenged *Atg5*$^{fl/fl}$ controls. In contrast, the lungs of HDM-
374 challenged *Atg5*$^{fl/fl}$*-MRP8-Cre* mice that delete *Atg5* specifically in neutrophils accumulated
375 similar numbers of immune cells as HDM-challenged *Atg5*$^{fl/fl}$ controls (**Figures S2E**). Therefore,
376 ATG5 functions in lung macrophages and DCs, but not neutrophils, to control neutrophil
377 accumulation during HDM challenge.
378
379 We have previously reported that autophagy functions in macrophages independent of its role in
380 inhibiting inflammasome activation to suppresses the production of G-CSF and KC as well as
381 neutrophil recruitment to the lungs during *Mycobacterium tuberculosis* infection[72], however,
382 this role for autophagy has only been studied in the context of infection. To directly test if ATG5
383 is required in macrophages to suppress G-CSF and KC production following the noninfectious
384 HDM exposure, we differentiated bone marrow stem cells from *Atg5*$^{fl/fl}$*-LysM-Cre* and *Atg5*$^{fl/fl}$
385 mice into bone marrow derived macrophages (BMDM) by culturing *ex vivo* in the presence of
386 macrophage colony-stimulating factor (M-CSF). We treated the *Atg5*$^{fl/fl}$*-LysM-Cre* and *Atg5*$^{fl/fl}$
387 BMDMs with 200 µg HDM for 24 hours and measured the levels of G-CSF and KC secreted into
388 the media. The levels of G-CSF and KC produced by naïve macrophages from *Atg5*$^{fl/fl}$*-LysM-Cre*
389 and *Atg5*$^{fl/fl}$ mice was below the limit of detection. HDM treatment resulted in significantly higher
390 levels of G-CSF and KC secreted from *Atg5*$^{fl/fl}$*-LysM-Cre* macrophages compared to *Atg5*$^{fl/fl}$
391 macrophages **(Figures 4C)**. Therefore, ATG5 functions in macrophages to suppress G-CSF and
392 KC production following direct sensing of PAMPs in HDM, which could otherwise promote
393 neutrophil accumulation in lungs.
394
395 **Autophagy is required in innate immune cells to control neutrophil-dominated inflammation**
396 **during HDM challenge**
397 ATG5 has been shown to control inflammatory responses via both autophagy-dependent and
398 autophagy-independent pathways[21,41–43,72–75]. To determine whether the regulation of
399 neutrophil recruitment and inflammation by ATG5 in HDM-challenged mice was dependent on
400 other autophagy proteins or represented an autophagy-independent role for ATG5, we monitored
401 neutrophil abundance in the lungs of mice lacking expression of the essential autophagy genes
402 *Atg16l1*, *Becn1, or Fip200* in $LysM^+$ cells following HDM challenge by flow cytometry.

403 BECLIN1 (encoded by *Becn1*) and FIP200 operate during the nucleation step of the
404 autophagosome membrane biogenesis, whereas ATG16L1 functions with ATG5 in the
405 phagophore elongation complex[25]. Similar to as observed in *Atg5*$^{fl/fl}$*-LysM-Cre* mice, HDM-
406 challenged *Atg16l1*$^{fl/fl}$*-LysM-Cre, Becn1*$^{fl/fl}$*-LysM-Cre*, and *Fip200*$^{fl/fl}$*-LysM-Cre* mice accumulated
407 more neutrophils and activated CD4^{+} T cells in their lungs compared to HDM-challenged
408 *Atg16l1*$^{fl/fl}$, *Becn1*$^{fl/fl}$, and *Fip200*$^{fl/fl}$ controls, respectively **(Figures 5A-B)**. The lungs of HDM-
409 challenged *Atg16l1*$^{fl/fl}$*-LysM-Cre* and *Fip200*$^{fl/fl}$*-LysM-Cre* mice also accumulated significantly
410 higher numbers of non-alveolar macrophages, DCs, and T_{regs} in comparison to HDM-challenged
411 *Atg16l1*$^{fl/fl}$ and *Fip200*$^{fl/fl}$ controls, respectively **(Figures 5C-E)**. The lungs of HDM-challenged
412 *Becn1*$^{fl/fl}$*-LysM-Cre* mice also accumulated a higher number of inflammatory monocytes compared
413 to HDM-challenged *Becn1*$^{fl/fl}$ mice **(Figures 5F)**. Similar to *Atg5*$^{fl/fl}$*-LysM-Cre* mice, we did not
414 observe differences in eosinophils in the HDM-challenged *Atg16l1*$^{fl/fl}$*-LysM-Cre*, *Becn1*$^{fl/fl}$*-LysM-*
415 *Cre*, and *Fip200*$^{fl/fl}$*-LysM-Cre* mice compared to controls **(Figure 5G)**. While ATG5, ATG16L1,
416 and BECLIN1 are essential for both canonical autophagy as well as the non-canonical autophagy
417 processes LC3 associated phagocytosis (LAP) and LC3-dependent endocytosis (LANDO), FIP200
418 is dispensable for the LAP and LANDO pathways. Therefore, the requirement for ATG5,
419 ATG16L1, BECLIN1, and FIP200 implies that canonical autophagy is necessary in LysM^{+} innate
420 immune cells to suppress the accumulation of neutrophils in the lungs of mice following HDM
421 challenge.
422
423 Together, our data supports a model where during airway exposure to allergens, ATG5 functions
424 in lung macrophages and DCs to tip the balance of T cell responses to favor T_H2 responses and
425 suppress T_H17 responses (**Figure 5H**). In addition, ATG5 is required in macrophages to inhibit
426 the secretion of cytokines and chemokines that can recruit neutrophils to the lungs during allergen
427 exposure in a T cell-independent manner. Therefore, ATG5 plays multiple roles in lung innate
428 immune cells to limit the neutrophil recruitment and mucus accumulation that would be associated
429 with severe asthma.
430
431 **DISCUSSION**

432 The association of genetic polymorphisms in the *ATG5* gene with susceptibility to asthma in
433 humans has drawn attention to the roles for autophagy in regulating inflammatory responses during
434 allergen challenge and asthma. In the present study, we directly investigate the roles for ATG5 and
435 autophagy in innate immune cells during asthma using a series of conditional knockout mouse
436 lines and two murine models of allergic airway inflammation model. Our data support a model
437 where ATG5 functions in an autophagy-dependent process in CD11c$^+$ lung macrophages and/or
438 DCs to promote T_H2-associated eosinophil accumulation and suppress T_H17 responses in an
439 allergen-dependent manner. In addition to regulating T cell responses, we find that autophagy
440 functions in macrophages exposed to HDM to suppress the secretion of cytokines and chemokines
441 that would otherwise recruit neutrophils to the lungs, independent of T cell responses.

442 Our studies reveal a function for autophagy in innate immune cells that can promote T_H2 responses
443 while suppressing T_H17 responses, positioning autophagy as a central regulator of T cell
444 polarization during allergen exposure. There are multiple possible mechanisms by which
445 autophagy could be functioning in CD11c$^+$ DCs and lung macrophages to impact T cell
446 polarization during HDM challenge. Both DCs and lung macrophages are antigen-presenting cells
447 (APCs) that could serve to activate allergen specific CD4$^+$ T cells during asthma[76–78].
448 Autophagy plays a central role in transferring antigen to vesicles that contain MHC class II
449 molecules for antigen presentation to CD4$^+$ T cells[79,80]. In addition to direct roles in MHC class
450 II antigen presentation, autophagy also regulates the production of cytokines that can impact the
451 polarization of T cells during activation. Loss of autophagy can result in increased production of
452 IL-23 by macrophages and DCs[81], and IL-23 can induce the differentiation of T cells into T_H17
453 cells[82,83]. Loss of autophagy in macrophages also promotes pro-inflammatory M1-like
454 macrophage polarization in inflammatory conditions such as aging-associated hepatic injury and
455 obesity[73,84], and macrophage polarization can also impact T cell responses. M1-like
456 macrophages produce T_H1 associated cytokines (TNF-α, IL-6, IL-1β, and IL-23) and induce a
457 T_H1/T_H17 type inflammatory response, while M2-like macrophages produce type 2 cytokines (IL-
458 5 and IL-13), activating a T_H2 responses[85]. M1-like macrophages also express higher levels of
459 the transcription factor IRF5, which was demonstrated to drive T_H1/T_H17 responses in culture[86]
460 and deletion of *Irf5* in mice causes a reduction in IFN-γ, IL-17, and neutrophil recruitment in

461 HDM-challenged mice[87]. Therefore, autophagy in macrophages and DCs can drive differential
462 T cell responses via antigen presentation and the production of inflammatory signals.

463 Loss of autophagy in lung macrophages and DCs also resulted in the accumulation of T_{regs} in the
464 lungs following HDM challenge. Although T_{regs} are well-known to suppress the inflammatory
465 responses during asthma[88–91], T_{reg} accumulation is also reported to be increased during severe
466 asthma[92,93]. Transfer of purified T_H17 cells promoted the expansion of T_{regs} in mice[94].
467 Therefore, it is possible that the increased T_H17 responses directly contribute to the increase in
468 T_{regs} during HDM challenge of *Atg5*$^{fl/fl}$-*LysM-Cre* mice, which may serve as a countermeasure to
469 dampen the increased inflammatory response. Loss of autophagy in DCs is also associated with
470 dysregulated T_{reg} function in mice due to an accumulation of ADAM10 metalloprotease on the
471 surface of DCs in the absence of autophagy[95]. Accumulation of ADAM10 leads to cleavage of
472 ICOS-L, which is required for the efficient maturation of T_{regs} in steady state. Moreover, in the
473 absence of proper maturation, FOXP3$^+$CD25$^+$ T_{regs} transition to IL-17$^+$ CD4$^+$ T cells[95], which
474 may explain the increased IL-17 expression in T_{regs} that we observed in HDM-challenged *Atg5*$^{fl/fl}$-
475 *LysM-Cre* mice.

476 In addition to its role in regulating T cell polarization during allergen exposure, we find that
477 autophagy also functions in macrophages independent of T cells to suppress the production of
478 IFN-γ, G-CSF, and KC in response to HDM exposure. High levels of IFN-γ, G-CSF, and IL-8
479 (KC) have all been associated with neutrophilic inflammation, asthma progression, and severe
480 asthma in humans[15,96,97]. Autophagy has been reported to serve a similar role in lung
481 macrophages during *M. tuberculosis* infection[72], however, this was assumed to be a response to
482 the active infection. Our studies here show that autophagy more generally regulates the production
483 of neutrophil recruitment signals from macrophages during exposure to PAMPs. This is supported
484 by prior studies that autophagy-deficient BMDMs upregulated pro-inflammatory cytokine
485 production in response to LPS and IFN-γ[98]. HDM is a complex mix of bioactive molecules and
486 immune stimulatory molecules (including proteases and other allergens, β-glucans, and chitin
487 exoskeleton) that can directly be sensed by innate immune cells through several pattern recognition
488 receptors (TLR and CLR), NOD like receptors, and protease activated receptors[49–51]. In
489 addition, the residual LPS present in HDM is sensed by TLR4, where increased doses of LPS shift
490 the eosinophilic lung inflammation induced by LPS-free HDM to neutrophil-dominated

491 inflammation[46,48]. Indeed, mice deficient in *Myd88* and *Tlr4* were found to be protected from
492 HDM induced allergic response[99]. ATG5 has also been reported to directly interact with and
493 regulate MyD88 in mouse embryonic fibroblast (MEF) cells by preventing the formation of
494 MyD88 condensates that result in increased MyD88-TRAF6-NFκB signaling complex
495 activation[100]. In addition, autophagy suppresses pro-inflammatory responses in macrophages
496 through mitophagy[101–104], the clearance of damage-associated molecular patterns (DAMPs)
497 and PAMPs[105–107], and ER-phagy[108,109]. These roles for autophagy could also impact
498 neutrophil recruitment and accumulation in the lungs during HDM challenge. The increased
499 sensitization to PAMP signaling in the absence of autophagy could also be contributing to the
500 enhanced T_H17 responses where autophagy promotes T_H17 responses through increased IL-23
501 secretion in response to TLR agonists[81]. Given the similarities between the roles for autophagy
502 during *M. tuberculosis* infection and HDM challenge, it is also likely that autophagy also regulates
503 inflammation in a similar manner during other pulmonary inflammatory diseases. In addition, there
504 is evidence that autophagy may play similar roles in other tissues where autophagy in myeloid
505 cells alleviated intestinal inflammation and neutrophil accumulation during macrophage activation
506 syndrome and adherent-invasive *Escherichia coli* (AIEC) infection in mice[98]. These findings
507 highlight autophagy as a central regulator of inflammatory responses from innate and adaptive
508 immune cells in multiple tissues and diseases.

509 Human asthma is a heterogeneous condition characterized by multiple endotypes with distinct
510 cellular signatures[110]. Patients with T_H2-high versus T_H2-low endotypes respond differently to
511 corticosteroid treatments, which is associated with distinct and mixed granulocytic phenotypes. In
512 addition, there exists incredible heterogeneity in what environmental trigger causes asthma in
513 humans, which can also include viral infections. In our mouse models, we examined one example
514 each of T_H2-high and T_H2-low allergic airway responses. Using these models we have identified
515 a protective role for autophagy in controlling neutrophil accumulation during asthma, suggesting
516 that inducing autophagy may hold promise as a therapeutic for treating severe asthma cases.
517 Although this provides a starting point for understanding the role of autophagy in innate immune
518 cells during allergic airway inflammation, the application of these findings to the spectrum of
519 diversity observed in asthma cases in humans will still require expanding the complexity of the
520 system, a challenge for all animal models of human disease. In addition, the therapeutic potential

521 for targeting autophagy is currently limited by the absence of autophagy-specific inducers and the
522 multitude of diverse roles for canonical autophagy in eukaryotic cells. Therefore, the translation
523 of these findings to treatments will benefit from future studies into the effectors that function
524 downstream of autophagy to govern the immune responses during airway exposure to allergens.

525

526 **METHODS**

527 Mouse strains

528 All flox mice (*Atg5*$^{fl/fl}$, *Becn1*$^{fl/fl}$, *Atg16l1*$^{fl/fl}$) used in this study have been described
529 previously[39,44,111,112] and are maintained in an enhanced barrier facility. LysM-Cre (Jax
530 #004781), CD11c-Cre (Jax #007567), and MRP8-Cre (Jax #021614) mice from the Jackson
531 Laboratory were crossed to specific flox mice, respectively. *Atg5*$^{fl/fl}$*-LysM-Cre* and *Atg5*$^{fl/fl}$ mice
532 were crossed with *Casp1/11*$^{-/-}$ (Jax #016621) germline deletion mice to generate *Atg5*$^{fl/fl}$*-LysM-*
533 *Cre/Casp1/11*$^{-/-}$ and *Atg5*$^{fl/fl}$*/Casp1/11*$^{-/-}$ mice. *Atg5*$^{fl/fl}$*-LysM-Cre* and *Atg5*$^{fl/fl}$ mice were crossed
534 with *Il17a*^{eGFP} (Jax #018472) mice to generate *Atg5*$^{fl/fl}$*-LysM-Cre/Il17a*^{eGFP} and *Atg5*$^{fl/fl}$*/Il17a*^{eGFP}
535 mice. Adult male and female mice (aged 8–12 weeks) were used for the experiments. All
536 experiments were performed with respective littermate flox controls. All mice have been
537 backcrossed to C57BL/6J background. The mice were housed and bred at Washington University
538 in St. Louis in specific pathogen-free conditions in accordance with federal and university
539 guidelines. All procedures involving animals were conducted following National Institute of
540 Health guidelines and protocols were approved by the Institutional Animal Care and Use
541 Committee of Washington University in St. Louis. Animals were euthanized by CO_2 asphyxiation,
542 approved by Euthanasia of the American Veterinary Association.

543

544 Allergic airway inflammation models

545 Mice were used in an OVA model of airway allergic inflammation as described before, with few
546 modifications[45]. 8-12 week old sex matched mice were sensitized with 50 µg OVA (Sigma,
547 A5503-5G) complexed with aluminum hydroxide and magnesium hydroxide suspension (Imject™
548 Alum Adjuvant, Thermo scientific, 77161) on day 0, 4 and 14 intraperitoneally in 200 µl 1X PBS.
549 Mice were challenged with 1 mg OVA in PBS in 25 µl intranasally on days 20, 21, and 22. Mice
550 were sacrificed on day 23, and the whole lung (without the post-caval lobe) was processed for flow

551 cytometry analysis. For the HDM model of allergic airway inflammation, 8-12 week-old sex
552 matched mice were challenged with HDM as described previously[14]. Briefly, mice were
553 challenged intranasally with HDM (Greer Laboratories, NC9756554) in PBS (Gibco, 10010023).
554 The first primary dose of HDM (200 µg in 40 µl PBS) was administered on day 0 and two
555 secondary (100 µg in 20 µl PBS) doses were administered on days 7 and 14. Mice were sacrificed
556 on day 15 and the whole lung except the post-caval lobe was processed for the flow cytometry
557 experiments.
558
559 Flow cytometry
560 Mouse lungs were excised after PBS perfusion, placed in DMEM (Gibco, 12100046), minced
561 finely, and digested at 37ºC for an hour with mechanical disruption with a stir bar and enzymatic
562 digestion with collagenase D (Roche, 11088875103) and DNase I (Sigma, D4527). Digested tissue
563 was treated with ACK buffer (Life technologies, A1049201) to remove red blood cells and were
564 passed through a 70 µm cell strainer to generate single cell suspension in 1 ml of semi-facs buffer
565 (1X PBS pH 7.4 supplemented with 2% FBS and 2 mM EDTA). 100 µl of cells were stained with
566 Zombie-NIR before staining with the antibody cocktail mix. Cells were resuspended in semi-facs
567 buffer in the presence of Fc receptor blocking antibody (BioLegend, 101302) and stained with
568 antibodies at a 1:200 dilution with the myeloid or lymphoid antibody cocktails. The innate immune
569 cell staining antibody cocktail included the following antibodies: Ly6G-BV421 (Biolegend, 1A8),
570 SiglecF-BV480 (Biolegend, E50-2440(RUO), CD45-BV570 (Biolegend, 30-F11), CD11b-BV650
571 (Biolegend, M1/70), CD103-BV750 (Biolegend, M290), Ly6C-BV785 (Biolegend, HK1.4),
572 MHCII-SparkBlue550 (Biolegend, M5/114.15.2), CD64-PerCP-eFluor710 (Biolegend, X54-
573 5/7.1), MerTK-PE-Cy7 (Biolegend, DS5MMER), CD206-eF660 (AF647) (eBiosciences,
574 C068C2), CD11c-APC/Fire750 (Biolegend, N418). The lymphoid cell staining antibody cocktail
575 included the following antibodies: CD8α-Pacific blue (Biolegend, 53-6.7), CD44-BV510
576 (Biolegend, IM7), CD45-BV570 (Biolegend, 30-F11), CD19-BV605 (Biolegend, 6D5), CD11b-
577 BV650 (Biolegend, M1/70), NK1.1-BV785 (Biolegend, PK136), TCRβ-FITC (Biolegend, H57-
578 597), NKp46-PerCP-eFluor710 (eBiosciences, 29A1.4), CD62L-PE/Cy5 (Biolegend, MEL-14),
579 CD25-PE-Cy7 (Biolegend, PC61), and CD4-APC (Biolegend, 100516). For the intracellular
580 staining, surface-stained cells were fixed with 4% PFA before proceeding for intracellular staining
581 for the transcription factors. Cells were permeabilized with 1X FoxP3 permeabilization buffer

582 (Biolegend, 421403) and the intracellular staining is performed for the transcription factors using
583 fluorophore conjugated antibodies for RORγt-APC (eBiosciences, B2D), GATA3-APC
584 (Biolegend, 16E10A23), and T-bet-APC (Biolegend, 4B10), in separate panels, as per Biolegend's
585 instructions . To label immune cells in the airways before performing flow cytometry analysis,
586 mice were anesthetized with a ketamine-xylazine cocktail injected intraperitoneally. CD45.2-FITC
587 (Biolegend, 104) was administered intratracheally in the anesthetized mice to allow for airway
588 specific cell staining in the live mice for 30 minutes. Mice were then sacrificed, and total lungs
589 were collected and processed for immune cell staining as described above. The airway localized
590 immune cell populations were identified based on the CD45.2 antibody label. Flow cytometric
591 analysis was performed on a Cytek Aurora and data was analyzed with FlowJo software (Tree
592 Star). The gating strategies are shown in **Figure S3**.
593
594 <u>T cell depletion and IL-17 blocking experiments</u>
595 For T cell depletion experiment, 8-10-week-old sex-matched mice groups received antibodies
596 against either anti-rat isotype control or anti $CD4^+$ and $CD8^+$ neutralizing antibody. Mice were
597 injected with either 500 µg anti-rat isotype antibody or a combination of 250 µg each of αCD4
598 and αCD8 neutralizing antibodies in PBS intraperitoneally two days (day -2) before the first HDM
599 challenge and again on day 5 and day 12 during the ongoing HDM challenge on day 0, 7 and 14,
600 followed by the sacrifice on day 15. Separate groups of HDM-challenged mice received 500 µg of
601 isotype control antibodies on the same schedule to serve as controls. For IL-17 blocking, mice
602 were injected intraperitoneally with 100µg anti-mouse anti-IL17 blocking antibody on days -1, 1,
603 3, 5, 6, 8, 10, 12, and 13, together with i.n. HDM challenge on day 0, day 7 and day 15, followed
604 by sacrifice on day 15. Separate groups of HDM-challenged mice received 500 µg of isotype
605 control antibodies on the same schedule to serve as controls. Following sacrifice, whole lung
606 (without the post-caval lobe) is processed for flow cytometry and analysis.
607
608 <u>Histology experiments</u>
609 Unperfused intact lung lobes were harvested from the HDM challenged mouse. Lungs were fixed
610 in 4% paraformaldehyde for 24 hours before transferring to 1X PBS until further processing. All
611 the lung sections were processed for paraffin embedding, microtome sectioning, and stained
612 separately with hematoxylin and eosin (H&E) and periodic acid-schiff (PAS) stain at the Anatomy

613 and pathology core (AMP core) at Washington University in St. Louis. Slides were imaged using
614 the Zeiss Axioscan 7 at the Washington University Center for Cellular Imaging (WUCCI). Images
615 were analyzed using ImageJ Fiji software as described in **Figure S4**.
616
617 Cytokine bead array
618 For cytokine analysis, the post-caval lobe of the lungs was resuspended in PBS, homogenized by
619 bead beating. Homogenates were centrifuged to isolate the cell debris-free supernatant and
620 analyzed by BioPlex-Pro Mouse Cytokine 23-Plex Immunoassay (Bio-Rad, M60009RDPD).
621 Assay was performed as per manufacturer's instructions. Total protein concentration of the cell
622 debris-free supernatant was estimated using a Bicinchoninic Acid (BCA) Assay kit
623 (ThermoFisher, 23225). Bead array data is normalized to the total protein concentration of the
624 individual sample and represented as picogram (pg) per milligram (mg) of total protein.
625
626 BMDM treatment and cytokine analysis
627 8-12-week old sex matched mice were euthanized, followed by collection of the femur and tibia
628 bones. Bones were flushed with complete RPMI media (Gibco, 11875135) containing 10% FBS
629 (HiMedia, RM10432) three times to harvest the bone marrow stem cells. Red blood cells were
630 lysed by ACK lysis buffer, followed by washing with 1X PBS to retrieve purified bone marrow
631 cells. Bone marrow cells were differentiated in the presence of conditioned RPMI media
632 containing the macrophage colony-stimulating factor (M-CSF), for 6 days, with additional media
633 supplementation on day 3. After 6 days, supernatant containing the non-adherent cells was
634 removed and adherent cells were washed with PBS three times, before collecting the differentiated
635 macrophages for the experiment. Cultured bone marrow derived macrophages (BMDMs) were
636 seeded in 6 well plate and treated with either mock or with 200 µg/ml HDM in RPMI media for
637 24 hours. Post incubation, cell supernatant was collected, centrifuged, and filtered to remove any
638 cellular components. The cell-free supernatant was used to analyze G-CSF and KC by ELISA
639 (R&D systems, DY414-05 for G-CSF and DY453-05 for KC) as per manufacturer's guidelines.
640
641 Statistical analysis for biological experiments
642 All the data from mouse experiments is from at least two independent experiments, unless
643 specified otherwise. Samples represent biological (not technical) replicates of mice randomly

644 sorted into each experimental group. No blinding was performed during animal experiments. If
645 presented on a log scale, the data was log transformed before statistical analysis. Statistical
646 differences were calculated using Prism 9.0 (GraphPad Software) using either unpaired Welch's
647 t-tests or one-way ANOVA or two-way ANOVA test with or without corrections as denoted in the
648 figure legends. Statistically significant differences are shown for comparisons within a genotype
649 or within treatment groups. Sample sizes were sufficient to detect differences as small as 10%
650 using the statistical methods described. When used, center values and error bars represent means
651 ± S.E.M. $P < 0.05$ was considered significant. $P < 0.05$ was denoted *, ** for $P < 0.01$, ***
652 $P < 0.001$, and **** $P < 0.0001$. Statistical test details aad outcomes for each comparison for all
653 graphs are available in Supplementary Dataset 1.
654

655 **AUTHOR CONTRIBUTIONS**

656 N.D. and C.L.S. designed the project, analyzed the data, and wrote the manuscript. N.D., S.V.H.,
657 S.R.M., N.R.E., R.L.K., S.K.N., M. S., and R.W. performed the experiments. N.D., A.R., A.L.K,
658 and C.L.S. designed the asthma protocols. A.S. assisted with the flow cytometry experiments and
659 analysis. D.K. maintained and bred the mouse lines. A.L.K. and C.L.S. advised project design. All
660 authors read and edited the manuscript.
661

662 **ACKNOWLEDGEMENTS**

663 This work was supported by NIH grants R01 AI132697, U19 AI142784, Burroughs Wellcome
664 Fund Investigators in the Pathogenesis of Infectious Disease, and the Philip and Sima Needleman
665 Center for Autophagy Therapeutics and Research to C.L.S. N.D. is supported by Alexander and
666 Gertrude Berg fellowship and S.K.N. is supported by a Stephen I. Morse Fellowship from the
667 Department of Molecular Microbiology at Washington University in St. Louis School of Medicine.
668 S.V.H. is supported by NIH grant T32 GM007067. R.L.K. is supported by a Potts Memorial
669 Foundation postdoctoral fellowship. This material is based upon work supported by the National
670 Science Foundation Graduate Research Fellowship Program under Grant #DGE 2139839 to
671 N.R.E. Flow cytometry was performed at the cWIDR and Department of Molecular Microbiology
672 Flow Cytometry Facility at Washington University School of Medicine. Histology slides were
673 imaged at the Washington University Center for Cellular Imaging (WUCCI), which is supported
674 by Washington University School of Medicine, the Children's Discovery Institute of Washington

University and St. Louis Children's Hospital (CDI-CORE-2015-505 and CDI-CORE-2019-813), and the Foundation for Barnes-Jewish Hospital (3770). Histology sections were processed and stained at the Anatomy and Pathology Core (AMP core) at Washington University in St. Louis, School of Medicine. Any opinions, findings, and conclusions or recommendations expressed in this material are those of the author(s) and do not necessarily reflect the views of the National Science Foundation.

DISCLOSURE STATEMENT

No potential conflict of interest was reported by the authors.

REFERENCES

[1] GBD 2019 Diseases and Injuries Collaborators. Global burden of 369 diseases and injuries in 204 countries and territories, 1990-2019: a systematic analysis for the Global Burden of Disease Study 2019. Lancet. 2020;396(10258):1204–1222.

[2] Papi A, Brightling C, Pedersen SE, et al. Asthma. Lancet. 2018;391(10122):783–800.

[3] Platts-Mills TAE, Woodfolk JA. Allergens and their role in the allergic immune response. Immunol Rev. 2011;242(1):51–68.

[4] Walford HH, Doherty TA. Diagnosis and management of eosinophilic asthma: a US perspective. J Asthma Allergy. 2014;7:53–65.

[5] Lambrecht BN, Hammad H, Fahy JV. The Cytokines of Asthma. Immunity. 2019;50(4):975–991.

[6] Bartemes KR, Kita H. Dynamic role of epithelium-derived cytokines in asthma. Clin Immunol. 2012;143(3):222–235.

[7] Haldar P, Pavord ID. Noneosinophilic asthma: a distinct clinical and pathologic phenotype. J Allergy Clin Immunol. 2007;119(5):1043–1052; quiz 1053–1054.

[8] Moore WC, Meyers DA, Wenzel SE, et al. Identification of asthma phenotypes using cluster analysis in the Severe Asthma Research Program. Am J Respir Crit Care Med. 2010;181(4):315–323.

[9] Robinson D, Humbert M, Buhl R, et al. Revisiting Type 2-high and Type 2-low airway inflammation in asthma: current knowledge and therapeutic implications. Clin Exp Allergy. 2017;47(2):161–175.

[10] Ray A, Kolls JK. Neutrophilic Inflammation in Asthma and Association with Disease Severity. Trends Immunol. 2017;38(12):942–954.

707 [11] Zhang X, Xu Z, Wen X, et al. The onset, development and pathogenesis of severe neutrophilic
708 asthma. Immunol Cell Biol. 2022;100(3):144–159.

709 [12] Newcomb DC, Peebles RS. Th17-mediated inflammation in asthma. Curr Opin Immunol.
710 2013;25(6):755–760.

711 [13] McKinley L, Alcorn JF, Peterson A, et al. TH17 cells mediate steroid-resistant airway
712 inflammation and airway hyperresponsiveness in mice. J Immunol. 2008;181(6):4089–4097.

713 [14] Suzuki Y, Maazi H, Sankaranarayanan I, et al. Lack of autophagy induces steroid-resistant airway
714 inflammation. J Allergy Clin Immunol. 2016;137(5):1382-1389.e9.

715 [15] Raundhal M, Morse C, Khare A, et al. High IFN-γ and low SLPI mark severe asthma in mice and
716 humans. J Clin Invest. 2015;125(8):3037–3050.

717 [16] Wisniewski JA, Muehling LM, Eccles JD, et al. TH1 signatures are present in the lower airways of
718 children with severe asthma, regardless of allergic status. J Allergy Clin Immunol.
719 2018;141(6):2048-2060.e13.

720 [17] Al-Ramli W, Préfontaine D, Chouiali F, et al. T(H)17-associated cytokines (IL-17A and IL-17F) in
721 severe asthma. J Allergy Clin Immunol. 2009;123(5):1185–1187.

722 [18] Poon AH, Chouiali F, Tse SM, et al. Genetic and histologic evidence for autophagy in asthma
723 pathogenesis. J Allergy Clin Immunol. 2012;129(2):569–571.

724 [19] Martin LJ, Gupta J, Jyothula SSSK, et al. Functional variant in the autophagy-related 5 gene
725 promotor is associated with childhood asthma. PLoS One. 2012;7(4):e33454.

726 [20] Pham DL, Kim S-H, Losol P, et al. Association of autophagy related gene polymorphisms with
727 neutrophilic airway inflammation in adult asthma. Korean J Intern Med. 2016;31(2):375–385.

728 [21] Kimmey JM, Huynh JP, Weiss LA, et al. Unique role for ATG5 in neutrophil-mediated
729 immunopathology during M. tuberculosis infection. Nature. 2015;528(7583):565–569.

730 [22] Kinsella RL, Nehls EM, Stallings CL. Roles for Autophagy Proteins in Immunity and Host Defense.
731 Vet Pathol. 2018;55(3):366–373.

732 [23] Kimmey JM, Stallings CL. Bacterial Pathogens versus Autophagy: Implications for Therapeutic
733 Interventions. Trends Mol Med. 2016;22(12):1060–1076.

734 [24] Lamb CA, Yoshimori T, Tooze SA. The autophagosome: origins unknown, biogenesis complex.
735 Nat Rev Mol Cell Biol. 2013;14(12):759–774.

736 [25] Mizushima N, Noda T, Yoshimori T, et al. A protein conjugation system essential for autophagy.
737 Nature. 1998;395(6700):395–398.

738 [26] Mizushima N, Yoshimori T, Ohsumi Y. The role of Atg proteins in autophagosome formation.
739 Annu Rev Cell Dev Biol. 2011;27:107–132.

740 [27] Li BB, Chen YL, Pang F. MicroRNA-30a Targets ATG5 and Attenuates Airway Fibrosis in Asthma
741 by Suppressing Autophagy. Inflammation. 2020;43(1):44–53.

742 [28] McAlinden KD, Deshpande DA, Ghavami S, et al. Autophagy Activation in Asthma Airways
743 Remodeling. Am J Respir Cell Mol Biol. 2019;60(5):541–553.

744 [29] Poon AH, Choy DF, Chouiali F, et al. Increased Autophagy-Related 5 Gene Expression Is
745 Associated with Collagen Expression in the Airways of Refractory Asthmatics. Front Immunol.
746 2017;8:355.

747 [30] Ban G-Y, Pham DL, Trinh THK, et al. Autophagy mechanisms in sputum and peripheral blood
748 cells of patients with severe asthma: a new therapeutic target. Clin Exp Allergy. 2016;46(1):48–
749 59.

750 [31] Theofani E, Xanthou G. Autophagy: A Friend or Foe in Allergic Asthma? Int J Mol Sci.
751 2021;22(12):6314.

752 [32] Liu J-N, Suh D-H, Trinh HKT, et al. The role of autophagy in allergic inflammation: a new target
753 for severe asthma. Exp Mol Med. 2016;48(7):e243.

754 [33] Schrezenmeier E, Dörner T. Mechanisms of action of hydroxychloroquine and chloroquine:
755 implications for rheumatology. Nat Rev Rheumatol. 2020;16(3):155–166.

756 [34] Das M, Ram A, Ghosh B. Luteolin alleviates bronchoconstriction and airway hyperreactivity in
757 ovalbumin sensitized mice. Inflamm Res. 2003;52(3):101–106.

758 [35] Kim S-H, Saba E, Kim B-K, et al. Luteolin attenuates airway inflammation by inducing the
759 transition of CD4+CD25- to CD4+CD25+ regulatory T cells. Eur J Pharmacol. 2018;820:53–64.

760 [36] Wang S, Wuniqiemu T, Tang W, et al. Luteolin inhibits autophagy in allergic asthma by activating
761 PI3K/Akt/mTOR signaling and inhibiting Beclin-1-PI3KC3 complex. Int Immunopharmacol.
762 2021;94:107460.

763 [37] Gu W, Cui R, Ding T, et al. Simvastatin alleviates airway inflammation and remodelling through
764 up-regulation of autophagy in mouse models of asthma. Respirology. 2017;22(3):533–541.

765 [38] McKay A, Leung BP, McInnes IB, et al. A novel anti-inflammatory role of simvastatin in a murine
766 model of allergic asthma. J Immunol. 2004;172(5):2903–2908.

767 [39] Wang Y-T, Zaitsev K, Lu Q, et al. Author Correction: Select autophagy genes maintain quiescence
768 of tissue-resident macrophages and increase susceptibility to Listeria monocytogenes. Nat
769 Microbiol. 2021;6(7):972.

770 [40] Lu Q, Yokoyama CC, Williams JW, et al. Homeostatic Control of Innate Lung Inflammation by Vici
771 Syndrome Gene Epg5 and Additional Autophagy Genes Promotes Influenza Pathogenesis. Cell
772 Host Microbe. 2016;19(1):102–113.

773 [41] Zhao Z, Fux B, Goodwin M, et al. Autophagosome-independent essential function for the
774 autophagy protein Atg5 in cellular immunity to intracellular pathogens. Cell Host Microbe.
775 2008;4(5):458–469.

776 [42] Galluzzi L, Green DR. Autophagy-Independent Functions of the Autophagy Machinery. Cell.
777 2019;177(7):1682–1699.

778 [43] Choi J, Park S, Biering SB, et al. The parasitophorous vacuole membrane of Toxoplasma gondii is
779 targeted for disruption by ubiquitin-like conjugation systems of autophagy. Immunity.
780 2014;40(6):924–935.

781 [44] Hara T, Nakamura K, Matsui M, et al. Suppression of basal autophagy in neural cells causes
782 neurodegenerative disease in mice. Nature. 2006;441(7095):885–889.

783 [45] Jaeger N, McDonough RT, Rosen AL, et al. Airway Microbiota-Host Interactions Regulate
784 Secretory Leukocyte Protease Inhibitor Levels and Influence Allergic Airway Inflammation. Cell
785 Rep. 2020;33(5):108331.

786 [46] Zhao S, Jiang Y, Yang X, et al. Lipopolysaccharides promote a shift from Th2-derived airway
787 eosinophilic inflammation to Th17-derived neutrophilic inflammation in an ovalbumin-sensitized
788 murine asthma model. J Asthma. 2017;54(5):447–455.

789 [47] Hammad H, Chieppa M, Perros F, et al. House dust mite allergen induces asthma via Toll-like
790 receptor 4 triggering of airway structural cells. Nat Med. 2009;15(4):410–416.

791 [48] Daan de Boer J, Roelofs JJTH, de Vos AF, et al. Lipopolysaccharide inhibits Th2 lung inflammation
792 induced by house dust mite allergens in mice. Am J Respir Cell Mol Biol. 2013;48(3):382–389.

793 [49] Maeda K, Caldez MJ, Akira S. Innate immunity in allergy. Allergy. 2019;74(9):1660–1674.

794 [50] Jacquet A, Robinson C. Proteolytic, lipidergic and polysaccharide molecular recognition shape
795 innate responses to house dust mite allergens. Allergy. 2020;75(1):33–53.

796 [51] Jacquet A. Characterization of Innate Immune Responses to House Dust Mite Allergens: Pitfalls
797 and Limitations. Front Allergy. 2021;2:662378.

798 [52] Kim Y-K, Oh S-Y, Jeon SG, et al. Airway exposure levels of lipopolysaccharide determine type 1
799 versus type 2 experimental asthma. J Immunol. 2007;178(8):5375–5382.

800 [53] Manni ML, Trudeau JB, Scheller EV, et al. The complex relationship between inflammation and
801 lung function in severe asthma. Mucosal Immunol. 2014;7(5):1186–1198.

802 [54] Choy DF, Hart KM, Borthwick LA, et al. TH2 and TH17 inflammatory pathways are reciprocally
803 regulated in asthma. Sci Transl Med. 2015;7(301):301ra129.

804 [55] Li L, Huang L, Vergis AL, et al. IL-17 produced by neutrophils regulates IFN-gamma-mediated
805 neutrophil migration in mouse kidney ischemia-reperfusion injury. J Clin Invest.
806 2010;120(1):331–342.

807 [56] Shi Y, Shi G, Wan H, et al. Coexistence of Th1/Th2 and Th17/Treg imbalances in patients with
808 allergic asthma. Chin Med J (Engl). 2011;124(13):1951–1956.

809 [57] Zheng R, Wang F, Huang Y, et al. Elevated Th17 cell frequencies and Th17/Treg ratio are
810 associated with airway hyperresponsiveness in asthmatic children. J Asthma. 2021;58(6):707–
811 716.

812 [58] Huang F, Yin J-N, Wang H-B, et al. Association of imbalance of effector T cells and regulatory
813 cells with the severity of asthma and allergic rhinitis in children. Allergy Asthma Proc.
814 2017;38(6):70–77.

815 [59] Zhu J, Liu X, Wang W, et al. Altered expression of regulatory T and Th17 cells in murine bronchial
816 asthma. Exp Ther Med. 2017;14(1):714–722.

817 [60] Zou X-L, Chen Z-G, Zhang T-T, et al. Th17/Treg homeostasis, but not Th1/Th2 homeostasis, is
818 implicated in exacerbation of human bronchial asthma. Ther Clin Risk Manag. 2018;14:1627–
819 1636.

820 [61] Theofani E, Semitekolou M, Samitas K, et al. TFEB signaling attenuates NLRP3-driven
821 inflammatory responses in severe asthma. Allergy. 2022;77(7):2131–2146.

822 [62] Biasizzo M, Kopitar-Jerala N. Interplay Between NLRP3 Inflammasome and Autophagy. Front
823 Immunol. 2020;11:591803.

824 [63] Sun Q, Fan J, Billiar TR, et al. Inflammasome and autophagy regulation - a two-way street. Mol
825 Med. 2017;23:188–195.

826 [64] Kim RY, Pinkerton JW, Essilfie AT, et al. Role for NLRP3 Inflammasome-mediated, IL-1β-
827 Dependent Responses in Severe, Steroid-Resistant Asthma. Am J Respir Crit Care Med.
828 2017;196(3):283–297.

829 [65] Ma M, Li G, Qi M, et al. Inhibition of the Inflammasome Activity of NLRP3 Attenuates HDM-
830 Induced Allergic Asthma. Front Immunol. 2021;12:718779.

831 [66] Simpson JL, Phipps S, Baines KJ, et al. Elevated expression of the NLRP3 inflammasome in
832 neutrophilic asthma. Eur Respir J. 2014;43(4):1067–1076.

833 [67] Theofani E, Semitekolou M, Morianos I, et al. Targeting NLRP3 Inflammasome Activation in
834 Severe Asthma. J Clin Med. 2019;8(10):E1615.

835 [68] Ramos CDL, Canetti C, Souto JT, et al. MIP-1alpha[CCL3] acting on the CCR1 receptor mediates
836 neutrophil migration in immune inflammation via sequential release of TNF-alpha and LTB4. J
837 Leukoc Biol. 2005;78(1):167–177.

838 [69] Yamamoto N, Kawakami K, Kinjo Y, et al. Essential role for the p40 subunit of interleukin-12 in
839 neutrophil-mediated early host defense against pulmonary infection with Streptococcus
840 pneumoniae: involvement of interferon-gamma. Microbes Infect. 2004;6(14):1241–1249.

841 [70] Ralph BA, Lehoux M, Ostapska H, et al. The IL-1 Receptor Is Required to Maintain Neutrophil
842 Viability and Function During Aspergillus fumigatus Airway Infection. Front Immunol.
843 2021;12:675294.

844 [71] Jones MR, Simms BT, Lupa MM, et al. Lung NF-kappaB activation and neutrophil recruitment
845 require IL-1 and TNF receptor signaling during pneumococcal pneumonia. J Immunol.
846 2005;175(11):7530–7535.

847 [72] Kinsella RL, Kimmey JM, Smirnov A, et al. Autophagy prevents early proinflammatory responses
848 and neutrophil recruitment during Mycobacterium tuberculosis infection without affecting
849 pathogen burden in macrophages. PLoS Biol. 2023;21(6):e3002159.

850 [73] Liu K, Zhao E, Ilyas G, et al. Impaired macrophage autophagy increases the immune response in
851 obese mice by promoting proinflammatory macrophage polarization. Autophagy.
852 2015;11(2):271–284.

853 [74] Ye X, Zhou X-J, Zhang H. Exploring the Role of Autophagy-Related Gene 5 (ATG5) Yields
854 Important Insights Into Autophagy in Autoimmune/Autoinflammatory Diseases. Front Immunol.
855 2018;9:2334.

856 [75] Feng S, McNehlan ME, Kinsella RL, et al. Autophagy promotes efficient T cell responses to
857 restrict high-dose Mycobacterium tuberculosis infection in mice. Nat Microbiol. 2024;9(3):684–
858 697.

859 [76] Liu MC, Xiao HQ, Breslin LM, et al. Enhanced antigen presenting and T cell functions during late-
860 phase allergic responses in the lung. Clin Exp Allergy. 2018;48(3):334–342.

861 [77] VanHook AM. Macrophages present antigens in allergic asthma. Sci Signal.
862 2022;15(755):adf2043.

863 [78] Zhu X, Cui J, Yi L, et al. The Role of T Cells and Macrophages in Asthma Pathogenesis: A New
864 Perspective on Mutual Crosstalk. Mediators Inflamm. 2020;2020:7835284.

865 [79] Ghislat G, Lawrence T. Autophagy in dendritic cells. Cell Mol Immunol. 2018;15(11):944–952.

866 [80] Lee HK, Mattei LM, Steinberg BE, et al. In vivo requirement for Atg5 in antigen presentation by
867 dendritic cells. Immunity. 2010;32(2):227–239.

868 [81] Peral de Castro C, Jones SA, Ní Cheallaigh C, et al. Autophagy regulates IL-23 secretion and
869 innate T cell responses through effects on IL-1 secretion. J Immunol. 2012;189(8):4144–4153.

870 [82] Cheng S, Chen H, Wang A, et al. Blockade of IL-23 ameliorates allergic lung inflammation via
871 decreasing the infiltration of Tc17 cells. Arch Med Sci. 2016;12(6):1362–1369.

872 [83] Aggarwal S, Ghilardi N, Xie M-H, et al. Interleukin-23 promotes a distinct CD4 T cell activation
873 state characterized by the production of interleukin-17. J Biol Chem. 2003;278(3):1910–1914.

874 [84] Liu R, Cui J, Sun Y, et al. Autophagy deficiency promotes M1 macrophage polarization to
875 exacerbate acute liver injury via ATG5 repression during aging. Cell Death Discov. 2021;7(1):397.

876 [85] Luo M, Zhao F, Cheng H, et al. Macrophage polarization: an important role in inflammatory
877 diseases. Front Immunol. 2024;15:1352946.

878 [86] Krausgruber T, Blazek K, Smallie T, et al. IRF5 promotes inflammatory macrophage polarization
879 and TH1-TH17 responses. Nat Immunol. 2011;12(3):231–238.

880 [87] Oriss TB, Raundhal M, Morse C, et al. IRF5 distinguishes severe asthma in humans and drives
881 Th1 phenotype and airway hyperreactivity in mice. JCI Insight. 2017;2(10):e91019, 91019.

882 [88] Strickland DH, Stumbles PA, Zosky GR, et al. Reversal of airway hyperresponsiveness by
883 induction of airway mucosal CD4+CD25+ regulatory T cells. J Exp Med. 2006;203(12):2649–
884 2660.

885 [89] Wilson MS, Pesce JT, Ramalingam TR, et al. Suppression of murine allergic airway disease by IL-
886 2:anti-IL-2 monoclonal antibody-induced regulatory T cells. J Immunol. 2008;181(10):6942–
887 6954.

888 [90] Dembele M, Tao S, Massoud AH, et al. Tregitopes Improve Asthma by Promoting Highly
889 Suppressive and Antigen-Specific Tregs. Front Immunol. 2021;12:634509.

890 [91] Kearley J, Barker JE, Robinson DS, et al. Resolution of airway inflammation and hyperreactivity
891 after in vivo transfer of CD4+CD25+ regulatory T cells is interleukin 10 dependent. J Exp Med.
892 2005;202(11):1539–1547.

893 [92] Smyth LJC, Eustace A, Kolsum U, et al. Increased airway T regulatory cells in asthmatic subjects.
894 Chest. 2010;138(4):905–912.

895 [93] Lee J-H, Yu H-H, Wang L-C, et al. The levels of CD4+CD25+ regulatory T cells in paediatric
896 patients with allergic rhinitis and bronchial asthma. Clin Exp Immunol. 2007;148(1):53–63.

897 [94] Zhou Q, Hu Y, Howard OMZ, et al. In vitro generated Th17 cells support the expansion and
898 phenotypic stability of CD4(+)Foxp3(+) regulatory T cells in vivo. Cytokine. 2014;65(1):56–64.

899 [95] Niven J, Madelon N, Page N, et al. Macroautophagy in Dendritic Cells Controls the Homeostasis
900 and Stability of Regulatory T Cells. Cell Rep. 2019;28(1):21-29.e6.

901 [96] Hosoki K, Ying S, Corrigan C, et al. Analysis of a Panel of 48 Cytokines in BAL Fluids Specifically
902 Identifies IL-8 Levels as the Only Cytokine that Distinguishes Controlled Asthma from
903 Uncontrolled Asthma, and Correlates Inversely with FEV1. PLoS One. 2015;10(5):e0126035.

904 [97] Kim Y-M, Kim H, Lee S, et al. Airway G-CSF identifies neutrophilic inflammation and contributes
905 to asthma progression. Eur Respir J. 2020;55(2):1900827.

906 [98] Xu J, Kong L, Oliver BA, et al. Constitutively active autophagy in macrophages dampens
907 inflammation through metabolic and post-transcriptional regulation of cytokine production. Cell
908 Rep. 2023;42(7):112708.

909 [99] Phipps S, Lam CE, Kaiko GE, et al. Toll/IL-1 signaling is critical for house dust mite-specific helper
910 T cell type 2 and type 17 [corrected] responses. Am J Respir Crit Care Med. 2009;179(10):883–
911 893.

912 [100] Inomata M, Into T, Niida S, et al. Atg5 regulates formation of MyD88 condensed structures and
913 MyD88-dependent signal transduction. Biochem Biophys Res Commun. 2013;437(4):509–514.

914 [101] Harris J, Deen N, Zamani S, et al. Mitophagy and the release of inflammatory cytokines.
915 Mitochondrion. 2018;41:2–8.

916 [102] Lazarou M, Sliter DA, Kane LA, et al. The ubiquitin kinase PINK1 recruits autophagy receptors to
917 induce mitophagy. Nature. 2015;524(7565):309–314.

918 [103] Song Y, Zhou Y, Zhou X. The role of mitophagy in innate immune responses triggered by
919 mitochondrial stress. Cell Commun Signal. 2020;18(1):186.

920 [104] Killackey SA, Philpott DJ, Girardin SE. Mitophagy pathways in health and disease. J Cell Biol.
921 2020;219(11):e202004029.

922 [105] Pouwels SD, Heijink IH, van Oosterhout AJM, et al. A specific DAMP profile identifies
923 susceptibility to smoke-induced airway inflammation. Eur Respir J. 2014;43(4):1183–1186.

924 [106] Tang D, Kang R, Coyne CB, et al. PAMPs and DAMPs: signal 0s that spur autophagy and
925 immunity. Immunol Rev. 2012;249(1):158–175.

926 [107] Huang X, Tan X, Liang Y, et al. Differential DAMP release was observed in the sputum of COPD,
927 asthma and asthma-COPD overlap (ACO) patients. Sci Rep. 2019;9(1):19241.

928 [108] Chipurupalli S, Samavedam U, Robinson N. Crosstalk Between ER Stress, Autophagy and
929 Inflammation. Front Med (Lausanne). 2021;8:758311.

930 [109] Moretti J, Roy S, Bozec D, et al. STING Senses Microbial Viability to Orchestrate Stress-Mediated
931 Autophagy of the Endoplasmic Reticulum. Cell. 2017;171(4):809-823.e13.

932 [110] Wesolowska-Andersen A, Seibold MA. Airway molecular endotypes of asthma: dissecting the
933 heterogeneity. Curr Opin Allergy Clin Immunol. 2015;15(2):163–168.

934 [111] Hwang S, Maloney NS, Bruinsma MW, et al. Nondegradative role of Atg5-Atg12/ Atg16L1
935 autophagy protein complex in antiviral activity of interferon gamma. Cell Host Microbe.
936 2012;11(4):397–409.

937 [112] Gawriluk TR, Hale AN, Flaws JA, et al. Autophagy is a cell survival program for female germ cells
938 in the murine ovary. Reproduction. 2011;141(6):759–765.

939

940

941 **FIGURE LEGENDS**

942 **Figure 1. ATG5 is required in LysM$^+$ cells to promote eosinophilia and to suppress**
943 **neutrophilia in airways following allergen exposure**
944 **(A)** Schematic of the OVA induced allergic airway inflammation model, made in part with
945 BioRender. (**B**) Representative flow gating of eosinophils as a frequency of CD45$^+$ cells in lungs
946 of *Atg5$^{fl/fl}$-LysM-Cre* and *Atg5$^{fl/fl}$* mice. **(C)** Number of neutrophils, eosinophils, non-alveolar
947 macrophages, DCs, total CD4$^+$ T cells, and activated CD4$^+$ T cells in the lungs of OVA-challenged
948 *Atg5$^{fl/fl}$-LysM-Cre* and *Atg5$^{fl/fl}$* mice, represented as cells per ml of lung suspension. **(D)** Number
949 of neutrophils and eosinophils in the airways of OVA-challenged *Atg5$^{fl/fl}$-LysM-Cre* and *Atg5$^{fl/fl}$*
950 mice, represented as cells per ml of lung suspension. **(E)** Schematic of the HDM-induced allergic
951 airway inflammation model, made in part with BioRender. (**F**) Representative flow gating of
952 neutrophils as a frequency of CD45$^+$ cells in lungs of *Atg5$^{fl/fl}$-LysM-Cre* and *Atg5$^{fl/fl}$* mice. **(G)**
953 Number of neutrophils, eosinophils, non-alveolar macrophages, DCs, inflammatory monocytes,
954 total CD4$^+$ T cells, activated CD4$^+$ T cells, and T_{regs} in the lungs of HDM-challenged *Atg5$^{fl/fl}$-LysM-*
955 *Cre* and *Atg5$^{fl/fl}$* mice, represented as cells per ml of the lung suspension. **(H)** Number of
956 neutrophils and eosinophils in the airways of the HDM-challenged *Atg5$^{fl/fl}$-LysM-Cre* and *Atg5$^{fl/fl}$*
957 mice, represented as cells per ml of lung suspension. **(I,K)** Lung sections from HDM-challenged
958 *Atg5$^{fl/fl}$-LysM-Cre* and *Atg5$^{fl/fl}$* mice stained with **(I)** H&E or **(K)** PAS stain. The boxed area in the
959 top panels is zoomed in on the bottom panels. **(J,L)** Quantification of area of **(J)** inflammation
960 based on nuclei area in H&E-stained lung histology sections and **(L)** mucus stain score calculated
961 by analyzing the total PAS-stained area normalized to total area of lung section. Each datapoint is
962 from an individual mouse. Data is presented on a $\log_{10}$ transformed scale except for panels J and
963 L. The bar graphs represent the mean +/- S.E.M. Unpaired Welch's t-test was used to determine
964 the statistical significance of differences and only the statistically significant differences are
965 shown. * $P < 0.05$, ** $P < 0.01$, *** $P < 0.001$, **** $P < 0.0001$.
966
967 **Figure 2. ATG5 expression in innate immune cells promotes T_H2 responses and suppresses**
968 **T_H17 responses during allergic airway inflammation**
969 **(A,C)** Number of total CD4$^+$ T cells in the lungs of **(A)** OVA- or **(C)** HDM-challenged *Atg5$^{fl/fl}$-*
970 *LysM-Cre* and *Atg5$^{fl/fl}$* mice, represented as cells per ml of the lung suspension. **(B,D)** Number of
971 CD4$^+$ T cells expressing RORγt, GATA3, or T-bet in the lungs of **(B)** OVA- or **(D)** HDM-
972 challenged *Atg5$^{fl/fl}$-LysM-Cre* and *Atg5$^{fl/fl}$* mice, represented as cells per ml of the lung suspension.

973 **(E)** Number of neutrophils and activated $CD4^+$ T cells in the lungs of HDM challenged *Atg5*$^{fl/fl}$-
974 *LysM-Cre/Il17a*^{eGFP} and *Atg5*$^{fl/fl}$/*Il17a*^{eGFP} mice, represented as cells per ml of the lung suspension.
975 **(F)** Percentage and **(G)** number of $CD4^+$ T cells, activated $CD4^+$ T cells, and T_{regs} expressing IL-
976 17A based on flow cytometry analysis of GFP expression in HDM-challenged *Atg5*$^{fl/fl}$*-LysM-*
977 *Cre/Il17a*^{eGFP} and *Atg5*$^{fl/fl}$/*Il17a*^{eGFP} mice. **(H)** Mean fluorescence intensity (MFI) of GFP (IL-17)
978 in $CD4^+$ T cells, activated $CD4^+$ T cells, and T_{regs}. **(I)** Ratio of the number of IL-17^+ $CD4^+$ T cells
979 to total T_{regs}. Legend for panel **E** also applies to panels **F-I**. Each datapoint is from an individual
980 mouse. **(A-E)** Data is presented on a $\log_{10}$ transformed scale. The bar graphs represent the mean
981 +/- S.E.M. **(A,C, E-I)** Unpaired Welch's t-test or **(B and D)** two-way ANOVA with Sidak's
982 correction was used to determine the statistical significance of differences between the groups and
983 only the statistically significant differences are shown. * $P < 0.05$, ** $P < 0.01$.
984
985 **Figure 3. Increased T_H17 responses in HDM-challenged *Atg5*$^{fl/fl}$*-LysM-Cre* mice are partially**
986 **responsible for the increased neutrophil accumulation**
987 **(A)** Schematic of time-course of antibody mediated depletion of T cells in a murine HDM model.
988 **(B-C)** Number of **(B)** T cells and (**C**) neutrophils in the lungs of HDM-challenged *Atg5*$^{fl/fl}$*-LysM-*
989 *Cre* and *Atg5*$^{fl/fl}$ mice that received either isotype control antibody or αCD4 and αCD8 antibodies,
990 represented as cells per ml of the lung suspension. **(D-F)** Concentration of (**D**) IL-17, (**E**) IFN-γ,
991 and (**F**) IL-5 in total lung homogenates from HDM-challenged *Atg5*$^{fl/fl}$*-LysM-Cre* and *Atg5*$^{fl/fl}$ mice
992 that received against either isotype control or αCD4 and αCD8 antibodies, based on cytokine bead
993 array. Only the data that is above the limit of detection is plotted, where # designates conditions
994 with samples below the limit of detection. Legend for panel B also applies to panels C-F. **(G)**
995 Schematic of time-course of the antibody mediated blocking of IL-17 in a murine HDM model.
996 (**H**) Number of neutrophils in the lungs of HDM-challenged *Atg5*$^{fl/fl}$*-LysM-Cre* and *Atg5*$^{fl/fl}$ mice
997 that received either isotype control antibody or αIL-17 blocking antibody. Each datapoint is from
998 an individual mouse. The bar graphs represent the mean +/- S.E.M. Two-way ANOVA with
999 Fisher's LSD test was used to determine the statistical significance of differences between the
1000 groups and statistically significant differences are shown for comparisons within a genotype or
1001 within treatment groups. * $P < 0.05$, ** $P < 0.01$, *** $P < 0.001$, **** $P < 0.0001$.
1002

1003 **Figure 4. ATG5 is required in macrophages to control the expression of neutrophil**
1004 **recruitment signals during exposure to HDM**
1005 (**A**) Concentration of G-CSF, KC, IL-1α, IL-12p40, and MIP-1α in total lung homogenate from
1006 HDM-challenged *Atg5*$^{fl/fl}$*-LysM-Cre* and *Atg5*$^{fl/fl}$ mice that received against either isotype control
1007 or αCD4 and αCD8 antibodies, from cytokine bead array. Only the data that is above the limit of
1008 detection is plotted. **(B)** Number of neutrophils, non-alveolar macrophages, DCs, inflammatory
1009 monocytes, activated CD4$^+$ T cells, T_{regs}, and eosinophils in the lungs of HDM-challenged *Atg5*$^{fl/fl}$-
1010 *CD11c-Cre* and *Atg5*$^{fl/fl}$ mice. Data is presented on a $\log_{10}$ transformed scale. **(C)** BMDMs were
1011 differentiated from bone marrow cells harvested from *Atg5*$^{fl/fl}$*-LysM-Cre* and *Atg5*$^{fl/fl}$ mice and
1012 treated with or without 200 µg HDM for 24 hours. Concentration of G-CSF and KC secreted into
1013 the media by ELISA. Each datapoint is from an individual mouse. The bar graphs represent the
1014 mean +/- S.E.M. Two-way ANOVA with Fisher's LSD test was used to determine the statistical
1015 significance of differences between the groups in panel A. Unpaired Welch's t-test was used to
1016 determine the statistical significance of differences between the groups for panels B and C. Only
1017 the statistically significant differences are shown in the graphs. * $P < 0.05$ and ** $P < 0.01$ *** P
1018 < 0.001.
1019
1020 **Figure 5. Autophagy is required in innate immune cells to control neutrophil-dominated**
1021 **inflammation during HDM-challenge**
1022 Number of **(A)** neutrophils (**B**) activated CD4$^+$ T cells, **(C)** non-alveolar macrophages, **(D)** DCs,
1023 **(E)** T_{regs}, (**F**) inflammatory monocytes, and (**G**) eosinophils in the lungs of HDM-challenged
1024 *Atg16l1*$^{fl/fl}$*-LysM-Cre*, *Atg16*$^{fl/fl}$, *Becn1*$^{fl/fl}$*-LysM-Cre*, *Becn1*$^{fl/fl}$, *Fip200*$^{fl/fl}$*-LysM-Cre*, and *Fip200*$^{fl/fl}$
1025 mice, represented as cells per ml of the lung suspension. Legends for panel A also applies to panel
1026 B-G. Each datapoint is from an individual mouse. Data is presented on a $\log_{10}$ transformed scale.
1027 The bar graphs represent the mean +/- S.E.M. Unpaired Welch's t-test was used to determine the
1028 statistical significance of differences between the groups, and only the statistically significant
1029 differences are shown. * $P < 0.05$, ** $P < 0.01$ *** $P < 0.001$. (**H**) Model for the roles of ATG5 in
1030 lung macrophages and DCs during allergic airway inflammation. The image is generated in part
1031 with BioRender.
1032

Figure 1

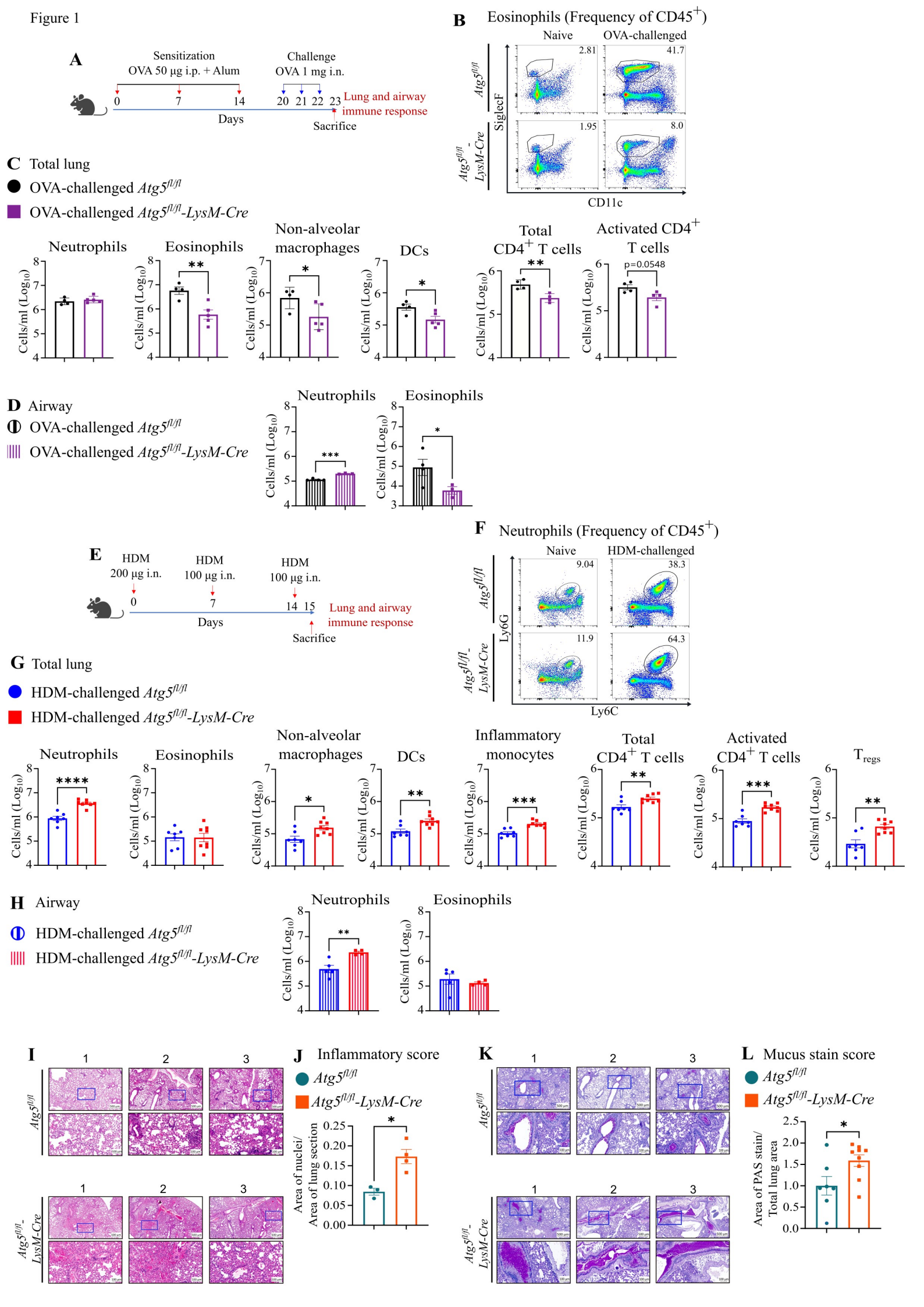
A
Sensitization
OVA 50 µg i.p. + Alum
Challenge
OVA 1 mg i.n.
0
7
14
20 21 22 23
Days
Lung and airway immune response
Sacrifice
B
Eosinophils (Frequency of CD45+)
Naive
OVA-challenged
Atg5fl/fl
Atg5fl/fl-LysM-Cre
SiglecF
CD11c
2.81
41.7
1.95
8.0
C Total lung
OVA-challenged Atg5fl/fl
OVA-challenged Atg5fl/fl-LysM-Cre
Neutrophils
Eosinophils
Non-alveolar macrophages
DCs
Total CD4+ T cells
Activated CD4+ T cells
Cells/ml (Log10)
p=0.0548
D Airway
OVA-challenged Atg5fl/fl
OVA-challenged Atg5fl/fl-LysM-Cre
E
HDM 200 µg i.n.
HDM 100 µg i.n.
HDM 100 µg i.n.
0
7
14 15
Days
Lung and airway immune response
Sacrifice
F Neutrophils (Frequency of CD45+)
Naive
HDM-challenged
9.04
38.3
11.9
64.3
Ly6G
Ly6C
G Total lung
HDM-challenged Atg5fl/fl
HDM-challenged Atg5fl/fl-LysM-Cre
Inflammatory monocytes
Tregs
H Airway
HDM-challenged Atg5fl/fl
HDM-challenged Atg5fl/fl-LysM-Cre
I
J Inflammatory score
Atg5fl/fl
Atg5fl/fl-LysM-Cre
Area of nuclei/ Area of lung section
K
L Mucus stain score
Atg5fl/fl
Atg5fl/fl-LysM-Cre
Area of PAS stain/ Total lung area

Figure 2

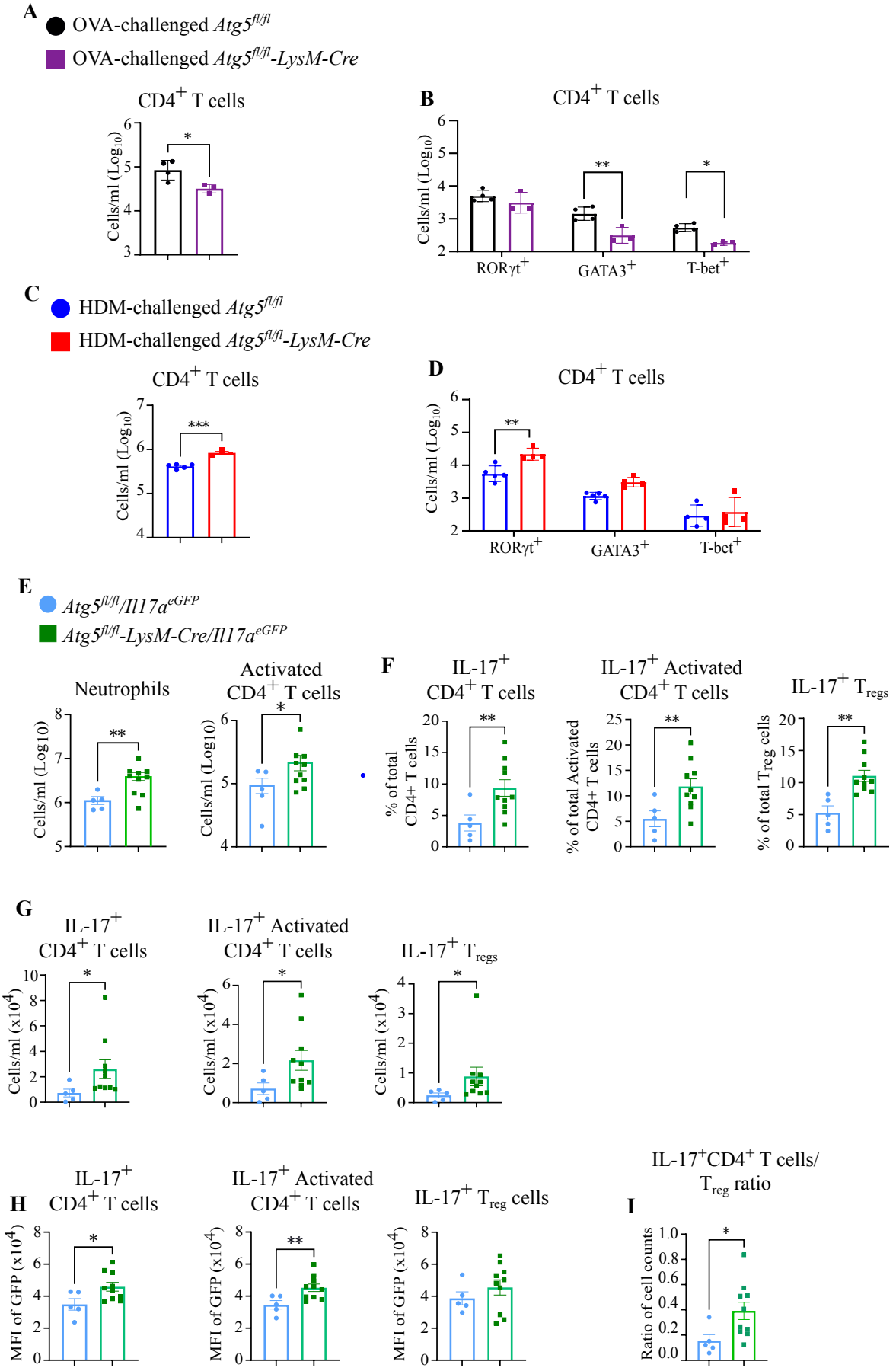
A
OVA-challenged Atg5fl/fl
OVA-challenged Atg5fl/fl-LysM-Cre
CD4+ T cells
Cells/ml (Log10)
B
CD4+ T cells
Cells/ml (Log10)
RORγt+
GATA3+
T-bet+
C
HDM-challenged Atg5fl/fl
HDM-challenged Atg5fl/fl-LysM-Cre
CD4+ T cells
Cells/ml (Log10)
D
CD4+ T cells
Cells/ml (Log10)
RORγt+
GATA3+
T-bet+
E
Atg5fl/fl/Il17aeGFP
Atg5fl/fl-LysM-Cre/Il17aeGFP
Neutrophils
Cells/ml (Log10)
Activated CD4+ T cells
Cells/ml (Log10)
F
IL-17+ CD4+ T cells
% of total CD4+ T cells
IL-17+ Activated CD4+ T cells
% of total Activated CD4+ T cells
IL-17+ Tregs
% of total Treg cells
G
IL-17+ CD4+ T cells
Cells/ml (x10^4)
IL-17+ Activated CD4+ T cells
Cells/ml (x10^4)
IL-17+ Tregs
Cells/ml (x10^4)
H
IL-17+ CD4+ T cells
MFI of GFP (x10^4)
IL-17+ Activated CD4+ T cells
MFI of GFP (x10^4)
IL-17+ Treg cells
MFI of GFP (x10^4)
I
IL-17+CD4+ T cells/ Treg ratio
Ratio of cell counts

Figure 3

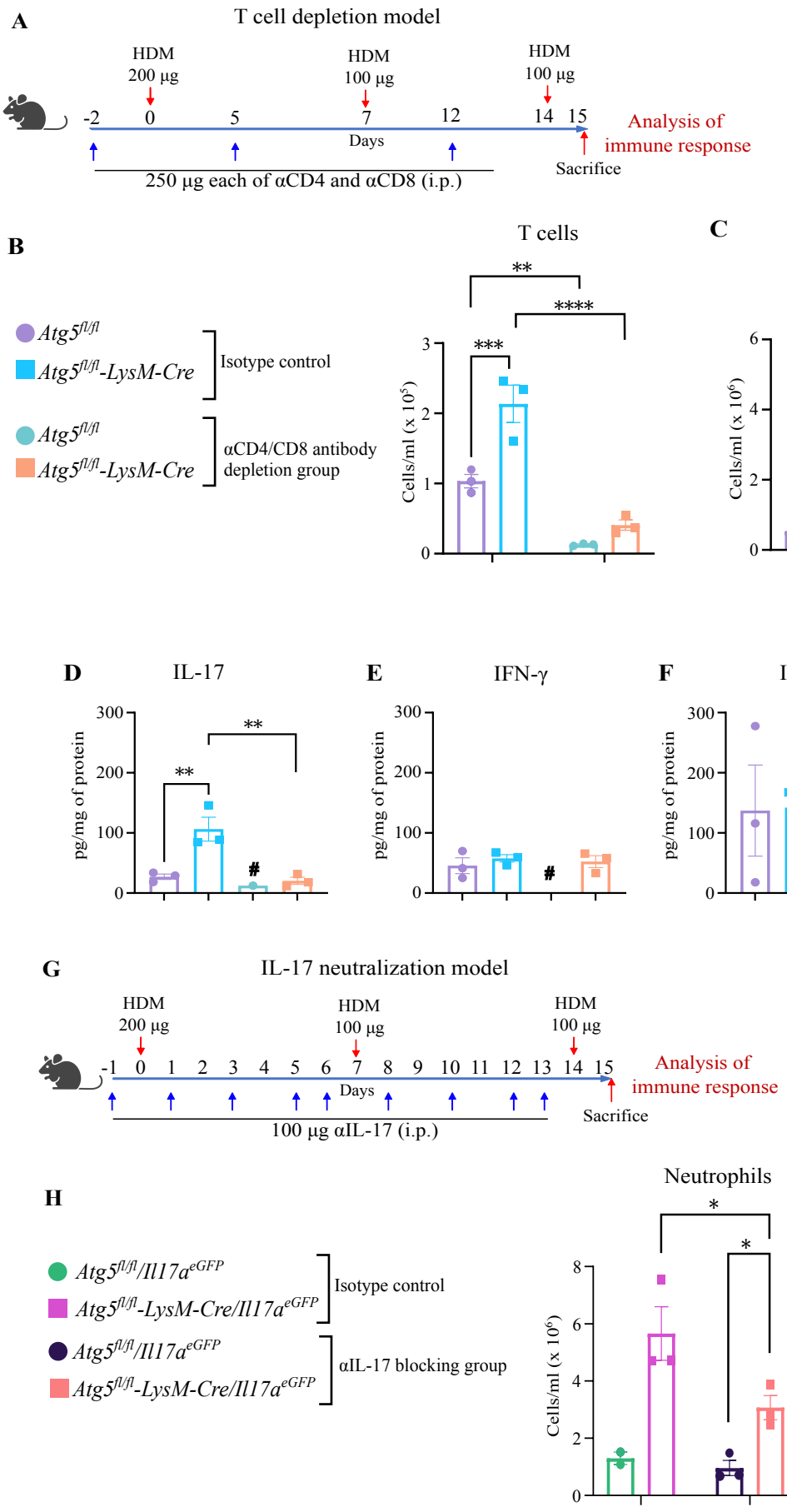
A
T cell depletion model
HDM 200 µg
HDM 100 µg
HDM 100 µg
-2 0 5 7 12 14 15
Days
Analysis of immune response
Sacrifice
250 µg each of αCD4 and αCD8 (i.p.)
B
Atg5fl/fl
Atg5fl/fl-LysM-Cre
Isotype control
Atg5fl/fl
Atg5fl/fl-LysM-Cre
αCD4/CD8 antibody depletion group
T cells
Cells/ml (x 10^5)
C
Neutrophils
Cells/ml (x 10^6)
D
IL-17
E
IFN-γ
F
IL-5
pg/mg of protein
G
IL-17 neutralization model
HDM 200 µg
HDM 100 µg
HDM 100 µg
-1 0 1 2 3 4 5 6 7 8 9 10 11 12 13 14 15
Days
Analysis of immune response
Sacrifice
100 µg αIL-17 (i.p.)
H
Atg5fl/fl/Il17aeGFP
Atg5fl/fl-LysM-Cre/Il17aeGFP
Isotype control
Atg5fl/fl/Il17aeGFP
Atg5fl/fl-LysM-Cre/Il17aeGFP
αIL-17 blocking group
Neutrophils
Cells/ml (x 10^6)

Figure 4

A

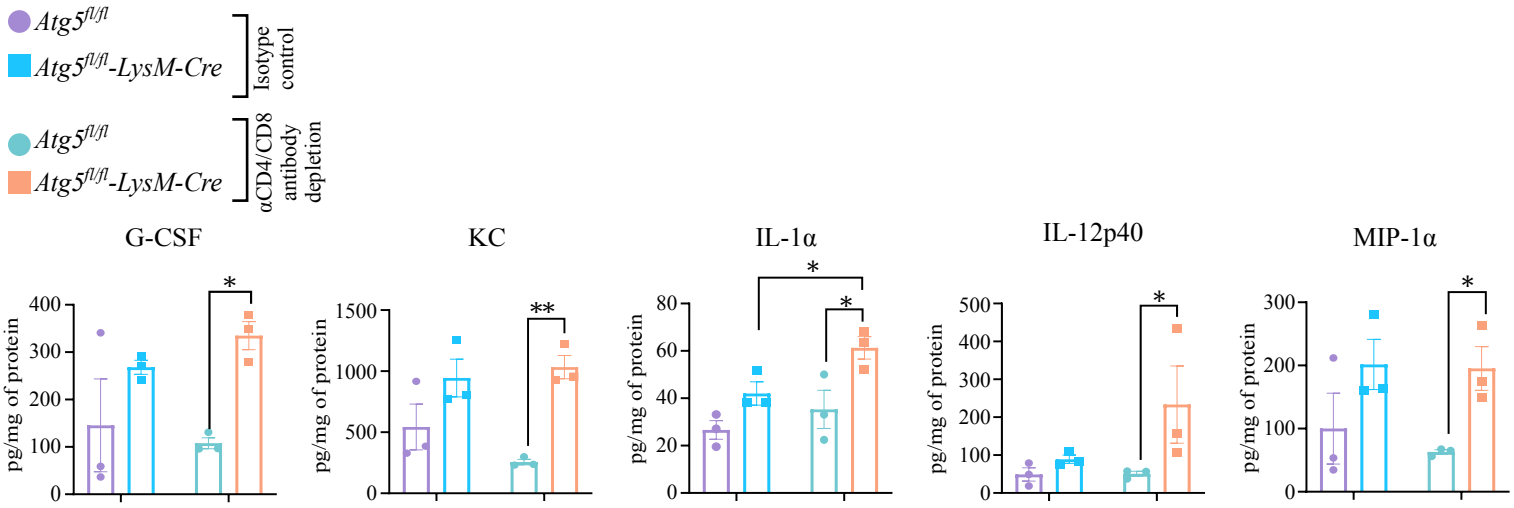
Atg5fl/fl
Atg5fl/fl-LysM-Cre
Isotype control
Atg5fl/fl
Atg5fl/fl-LysM-Cre
αCD4/CD8 antibody depletion
G-CSF
KC
IL-1α
IL-12p40
MIP-1α
pg/mg of protein

B

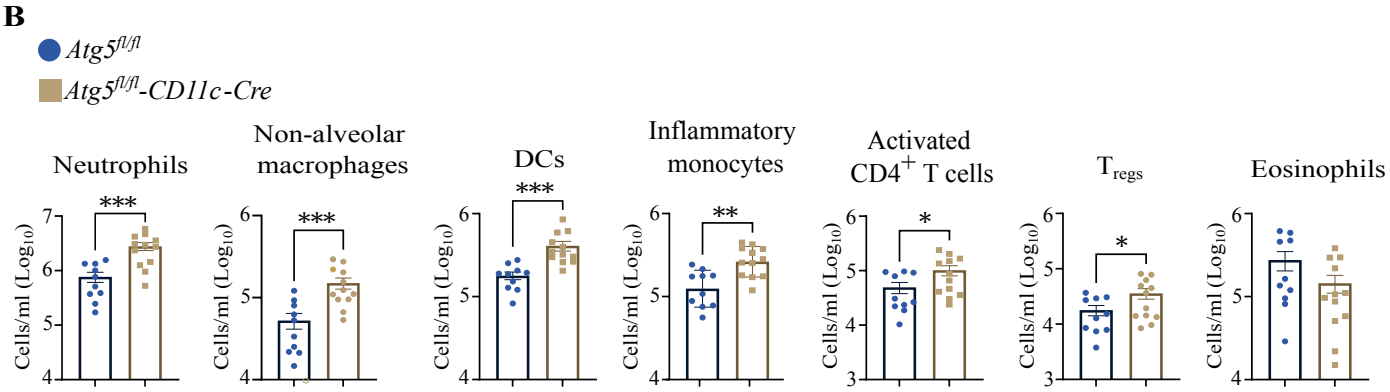
Atg5fl/fl
Atg5fl/fl-CD11c-Cre
Neutrophils
Non-alveolar macrophages
DCs
Inflammatory monocytes
Activated CD4+ T cells
Tregs
Eosinophils
Cells/ml (Log10)

C

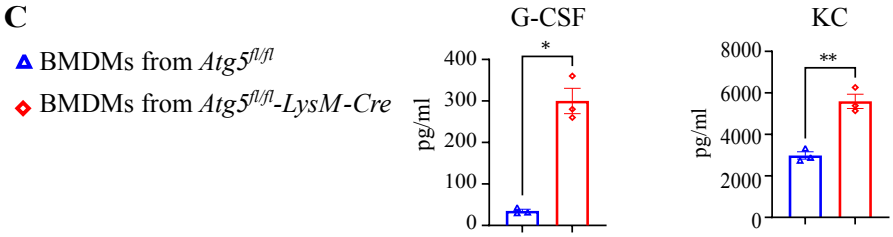
BMDMs from Atg5fl/fl
BMDMs from Atg5fl/fl-LysM-Cre
G-CSF
KC
pg/ml

Figure 5

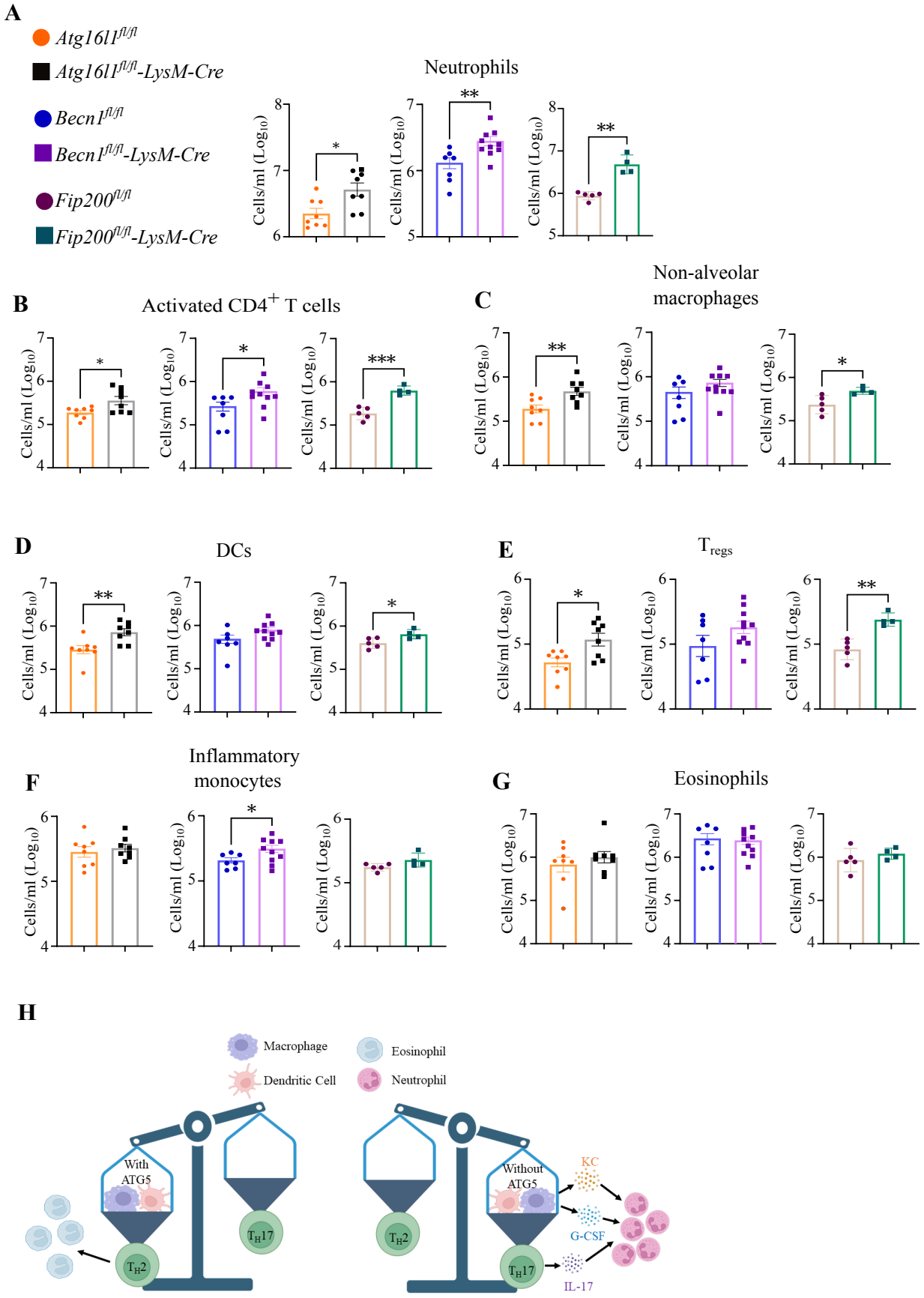
A
Atg16l1fl/fl
Atg16l1fl/fl-LysM-Cre
Becn1fl/fl
Becn1fl/fl-LysM-Cre
Fip200fl/fl
Fip200fl/fl-LysM-Cre
Neutrophils
Cells/ml (Log10)
B
Activated CD4+ T cells
C
Non-alveolar macrophages
D
DCs
E
Tregs
F
Inflammatory monocytes
G
Eosinophils
H
Macrophage
Dendritic Cell
Eosinophil
Neutrophil
With ATG5
Without ATG5
TH2
TH17
KC
G-CSF
IL-17